Nanoscale Advances

Accepted Manuscript

This article can be cited before page numbers have been issued, to do this please use: A. K. Chettupalli, S. P. N. Bukke, G. J. Udom, T. S. Saraswathi, S. A. Rahaman, S. N. Rai, M. Kavitha, N. Boggula, N. Goruntla, T. M. Yadesa and H. Onohuean, *Nanoscale Adv.*, 2024, DOI: 10.1039/D4NA00510D.

ROYAL SOCIETY OF CHEMISTRY

rsc.li/nanoscale-advances

View Article Online
DOI: 10.1039/D4NA00510D

Investigating New Bilosomes for *Ex vivo* Skin Deposition, *In Vitro* Characterization, and Transdermal Delivery of Nimodipine

Ananda Kumar Chettupalli[1], Sarad Pawar Naik Bukke[2], Godswill James Udom[3], Tenpattinam Shanmugam Saraswathi[4], Shaik Abdul Rahaman[1],* Sachchida Nand Rai[5], *Marati Kavitha[6], Narender Boggula[7], Narayana Goruntla[8], Tadele Mekuriya Yadesa[8]*, *Hope Onohuean[9]*

[1]Department of Pharmaceutical Siences, School of Pharmacy, Galgotias University, Greater Noida, Uttar Pradesh -203201, India

[2]Department of Pharmaceutics and Pharmaceutical Technology, Kampala International University, Western Campus, P.O.Box 71, Ishaka - Bushenyi, Uganda

[3]Department of Pharmacology and Toxicology, Kampala International University, Western Campus, P.O.Box 71, Ishaka - Bushenyi, Uganda

[4]Department of Pharmaceutics, SRM College of Pharmacy, SRM Institute of Science and Technology, Kattankulathur, Tamilnadu-603203, India

[5]Centre of Experimental Medicine and Surgery (CEMS), Institute of Medical Sciences (IMS), Banaras Hindu University (BHU), Varanasi-221005, Uttar Pradesh, India

[6]Department of Pharmacology, Raja Bahadur Venkata Rama Reddy (RBVRR) Women's College of Pharmacy, Barkatpura, Hyderabad, Telangana, India

[7]Department of Pharmaceutical Chemistry, CMR College of Pharmacy, Kandlakoya, Medchal, Hyderabad, Telangana, India – 501 401

[8]Department of Clinical Pharmacy and Pharmacy Practice, Kampala International University, Western Campus, P.O. Box 71, Ishaka-Bushenyi, Uganda

[9]Biopharmaceutic Unit, Department of Pharmacology and Toxicology, Kampala International University, Western Campus, P.O. Box 71, Ishaka-Bushenyi, Uganda

[*]**Correspondence**

Sarad Pawar Naik BUKKE, Department of Pharmaceutics and Pharmaceutical Technology, Kampala International University, Western Campus, P.O. Box 71, Ishaka - Bushenyi, Uganda drsaradpawar@kiu.ac.ug, https://orcid.org/0000-0002-5693-2953

View Article Online
DOI: 10.1039/D4NA00510D

Abstract

Background: This study developed and evaluated bilosomes containing Nimodipine (NDP) to create an appropriate formulation for a sustained-release transdermal gel.The generated bilosomal gel formulation was tested for its potential to increase NDP bioavailability and regulate its release from the transdermal gel dose form.This analysis included ex vivo, in vivo, and in vitro drug release trials.

Purpose: The objective of this work was to verify the validity of this notion by creating new nano bilosomes, modifying the composition of existing ones, and employing different bile salts as endogenous agents (EnAs). Subsequently, they sought to evaluate the efficacy of these novel bilosomes in comparison to a drug solution for the transdermal delivery of NDP.

Method: To find the best thin film hydration composition, bilosomes used a 33-factor design. This procedure utilizes Design Expert® software.We are creating and testing bilosomes with nimodipine to identify the optimal transdermal gel dose form that delivers the drug slowly and effectively while enhancing NDP bioavailability. We tested the medicine's transdermal gel release control in ex-vivo, in-vivo, and in-vitro trials.

Results: The NDP-bilosomes were tuned for a diameter of 136.48±7.82 nm, a surface charge of -48.37±0.49 mV, and an 88.56±1.73% drug encapsulation efficiency Their high negative zeta potential stabilized the compositions. TEM revealed spherical optimized vesicles. Bilosome biphasic NDP release validated Higuchi's theory. FTIR, DSC, and XRD showed that the lipid matrix included all NDP. NDP-Bilosomal gel has good pH, viscosity, consistency, and spreadability. In rats, NDP bilosomal gel showed higher peak plasma concentration and bioavailability than oral nimodipine solution, as indicated by a larger AUC0-∞. Both oral NDP suspension and NDP bilosomal gel had Cmax values of 52.37 and 215.39 µg/mL, respectively, 2 and 16 hours post-delivery. Transdermal bilosomal gel delivery led to increased NDP release, with an AUC0-∞ value of 67.21082238 (g.h/mL). After oral dosage,AUC was 0.439769476 g.h/mL from 0 to infinity (0-∞). The topical safety of F4 was tested on male Wistar rats using in vivo histopathology.

Conclusion: Bilosomes were better than drugs for increasing NDP flow over the skin,according to the study. The results showed that bilosomes increase NDP flow and that skin is better than drug solution.

View Article Online
DOI: 10.1039/D4NA00510D

Keywords: Bilosomes, Nimodipine, Transdermal-delivery, Edge-activators, Ex-vivo-permeation.

Introduction

Transdermal drug delivery (TDD) has become a highly attractive method to enhance the effectiveness of drugs that require significant hepatic processing when taken orally in recent decades[1]. TDDS enable controlled and prolonged release of drug, thereby reducing the adverse effects associated with conventional routes of administration [2,3]. TDDS formulation is highly challenging due to the barrier-like nature of the stratum corneum (SC), which consists of many lipid layers and hinders the penetration of most drugs into the skin. Various techniques such as chemical enhancers, supersaturation to increase thermodynamic activity, modification of the SC, physical methods like ultrasound and iontophoresis, and encapsulation in nanoparticles and vesicles have been employed to modify the skin barrier and facilitate drug delivery through the skin [4–6].

Researchers have shown tremendous interest in the TDDS due to the low permeability of the SC, which is the primary barrier for the absorption of external chemicals into the skin[7]. It functions as an alternative means of drug delivery. The intravenous method has several advantages compared to the oral route, such as preventing drug degradation and first-pass metabolism[8]. Vesicular systems have been employed to enhance drug permeability by modifying the stratum corneum and eliminating intercellular lipid barriers[9].

Nanovesicles provide a sophisticated method for delivering medications via the skin, thanks to their small size and the ability of some types to pass through the skin without breaking apart. They have been utilized for their capacity to enhance penetration and absorb at interfaces, as well as their ability to permeate the lipid structure of the stratum corneum (SC), thereby modifying its barrier function and facilitating the drug's partitioning into the skin [10,11]. Moreover, their lipid topologies enable them to make the SC bilayers more fluid, hence increasing the rate at which drugs can penetrate [12]. Vesicular systems are biodegradable, non-toxic, amphiphilic, and can modulate drug bioavailability [13]. They necessitate uncomplicated preparation protocols and might be enhanced by improving their composition [14,15]. They can change how drugs are absorbed through the skin by working as a matrix that breaks down drugs, a local storage area for long-term release, a barrier that lets dermally active compounds flow, or a membrane that slows the process [16]. Liposomes, niosomes, ethosomes, and transferosomes are known to carry tiny particles [17–22].

View Article Online
DOI: 10.1039/D4NA00510D

The choice of components in the vesicular system is crucial for enhancing drug penetration by disrupting the tight junctions of the SC [23]. Various lipid-based delivery methods, including bilosomes, ethosomes, niosomes, transferosomes, and liposomes, have been employed to improve the penetration and absorption of medicines with low solubility [24–28]. Bilosomes (BSs) are a type of vesicular drug carrier that contains bile salt. Sodium-deoxycholate, a negatively charged bile salt, improves the stability of BS and increases its capacity to pass through the stratum corneum of the skin by causing it to become more fluid [29]. Various bilosomes have been developed and assessed for in vitro and in vivo investigations [30–32]. The researchers have documented the presence of vesicles at the micro scale and observed an increase in the ability of tested medications to pass through and be released. In addition, vesicular systems can be included into hydrogel bases to enhance the distribution and stability of the formulation [33]. Natural or artificial cellulose polymers and carbomers make hydrogels. These bioadhesives, bilosome-compatible polymers increase medicine's solubility and delivery [34,35].

Nimodipine (NDP) is an orally administered drug that acts as a calcium channel blocker, primarily used for the treatment of hypertension. It attaches to the L-type voltage-gated calcium channel.The medicine is classified as a BCS (biopharmaceutical categorization system) class-II drug [36]. The drug's bioavailability was determined to be 13% following oral administration, with a half-life ranging from 8 to 9 hours. The administered oral dose is 60mg, while the intravenous dosage ranges from 1-2mg each hour. The molecular weight is 418.44 g/mol. The transdermal drug delivery system (TDDS) offers a solution for hypertension patients by addressing limitations and offering additional therapeutic advantage.[37]. NDP is suitable for transdermal dosageform because of its low molecular weight, high lipid solubility, fast elimination, and low oral bioavailability.

Therefore, the objective of this study was to determine the high level of flexibility of bilosomes in improving skin permeability compared to utilizing NDP as a model medication. In order to accomplish this objective, a comprehensive $3^1.2^2$ factorial design was utilized with the assistance of Design-Expert® software. This design was implemented to create bilosomes and investigate how various formulation variables impact the properties of the bilosomes. The ultimate aim was to identify the most desirable formula by utilizing the desirability function. Moreover, we conducted ex vivo permeation and in vivo skin deposition investigations on the most effective bilosomes, comparing them to a commercially available formulation and the drug suspension.

View Article Online
DOI: 10.1039/D4NA00510D

Furthermore, a histological examination was conducted on male Wistar rats to verify the safety of the bilosomes that were prepared.

Materials and Methods

Materials

Hetero Pharma Pvt Ltd, located in Hyderabad, Telangana, India, generously provided a gift sample of nimodipine. The following chemicals were acquired from Sigma-Aldrich (St. Louis, MO): Span 20® (sorbitan monolaurate), Span 40® (sorbitan monopalmitate), Span 60® (sorbitan monostearate), Carboxy methylcellulose (CMC), and cellulose membrane with a molecular weight cutoff of 12,000-14,000. The cholesterol PB (95%) (CH) was acquired from Alpha Chemika, located in Mumbai, India. The Sodium Deoxycholate (SDC) was acquired from BDH laboratory reagents in England. The chloroform used in this study was obtained from Alpha Chemical, a supplier based in Mumbai, India. The chloroform was of high-performance liquid chromatography (HPLC) grade. The potassium dihydrogen phosphate and disodium hydrogen phosphate were of high purity.

Preliminary Study

An initial investigation was conducted to determine the lower and upper values of the independent variables. The various formulations were created using surfactants, bile salts, and CH. The formulations were assessed for their size, polydispersity index (PDI), and encapsulation efficiency. The investigation commenced by utilizing the minimum concentration to initiate the formulation of bilosomes, which were then left undisturbed for a duration of 24 h to assess the development of a homogeneous phase. The occurrence of a homogeneous state did not happen at extremely low concentrations. The concentration of components was systematically increased to assess the development of bilosomes with a nano-size, low PDI, and optimal encapsulation. When the concentration is extremely high, bilosomes of larger size are generated, which have higher PDI. Therefore, the formulation of bilosomes selecting independent variables such as surfactants (span 20, span 40, and span 60) with surfactant:cholesterol ratios of 2:8, 1:1, and 8:2, as well as bile salt ranging from 5 to 20 mg. The methanol and chloroform mixture was chosen as the organic solvent due to its highest solubility of the components [38].

Preparation of NDP-loaded bilosomes

View Article Online
DOI: 10.1039/D4NA00510D

The thin film hydration (TFH) technique was used to prepare bilosomes loaded with NDP [39]. We created 10 mL of a chloroform-methanol (7:3) ratio after precisely measuring and dissolving bile salt (SDC), 40 mg of NDP, span 20, 40, 60 of surfactant, and CH. A rotating evaporator (Rotavapor, Heidolph VV 2000, Burladingen, Germany) slowly evaporated an organic solution in a 250-mL round-bottom flask with a long neck at 60 °C and 90 rpm for 30 min[40]. The flask was subjected to a vacuum for an additional 30 min to guarantee complete elimination of any residual solvents. The desiccated film was rehydrated by adding 10 mL of ultra-pure distilled water. The flask containing the film was then rotated in a water bath set at 60°C for 30 min at a speed of 150 rpm. This was done using the same equipment under standard atmospheric pressure. Glass beads were employed throughout the hydration process to enhance the yield of the produced nanovesicles. The resulting suspension of large multilamellar vesicles (LMVs) was subsequently transformed into small unilamellar vesicles (SUVs) using a 30-min sonication process using an Ultrasonic bath sonicator (Model SH 150-41; USA) at a temperature of 25°C. Afterwards, the refined dispersion was allowed to stabilize overnight at a temperature of 4°C to ensure that the vesicles fully merged and the drug was evenly distributed between the water-filled center and the lipid bilayer[5].

Experimental Design

A complete factorial design with 3^3 factors was implemented to investigate the impact of formulation variables on the NDP-loaded bilosomal dispersions. The Design-Expert® version 13.0.5.0 software (Stat-Ease, Inc., Minneapolis, MN, USA) was utilized for this purpose. The study design in Table I incorporated three formulation components as independent variables, each at three distinct levels. These factors were examined to determine their effects on four specific responses, which were considered as dependent variables. The experimental design was employed to examine the response surfaces of various independent components, resulting in a polynomial equation for the model and the numerical determination of many solutions for the optimal formulation[41]. A 3^3 complete factorial design was created to optimize the components listed below. The study investigated the effects of three factors, X1 (surfactant), X2 (surfactant to cholesterol ratio), and X3 (SDC in mg), on four dependent variables, Y1 (entrapment efficiency), Y2 (vesicle size), Y3 (PDI), and Y4 (zeta potential), as shown in Table 1. The data were subjected to a one-way analysis of variance (ANOVA) test in order to assess the importance of the factors being examined on the selected responses, as well as the interactions between these factors [42,43]. An

View Article Online
DOI: 10.1039/D4NA00510D

ANOVA was conducted on the experimental data to analyze the responses. The optimal model for each response variable, whether it is a main effect (one-factor effect), a 2-factor interaction (2FI), or a 3-factor interaction (3FI), is determined by estimating the statistical parameters, anticipated R^2, and the predicted residual error sum of squares (PRESS). Subsequently, an ANOVA statistical analysis was conducted to assess the significance of the effects of the tested factors and their interactions on the answers, using the best-fitted factorial model. A level of statistical significance was deemed significant at a P-value of less than 0.05.

Table 1. The optimization of bilosomes loaded with NDP was carried out using the Full Factorial Design 33.

Parameter	**Low (-1)**	**Medium (0)**	**High (+1)**
Independent Variables			
Surfactant Type (X1)	Span 20	Span 40	Span 60
Surfactant: Cholesterol (X2)	1:1	8:2	2:8
Sodium deoxycholate (X3)	5	10	20
Dependent variables			
Entrapment Efficiency (%)	Maximize		
Vesicle Size (nm)	Minimize		
PDI	Inrange		
Zetapotential (mV)	Maximize		

Investigation of Bilosomes Loaded with NDP

Finding the percentage of NDP entrapment efficiency

The Entrapment efficiency (EE%) of NDP was determined indirectly by quantifying the concentration of unentrapped NDP in the dispersion media [44]. The liberated NDP was isolated from the produced nanovesicles using centrifugation. Specifically, 1 mL of the vesicular suspension was subjected to centrifugation at 25000 rpm for 1 hour at 4°C using a cooling centrifuge. The resulting liquid that settled at the top was separated, appropriately thinned, and examined for the concentration of unbound nucleoside diphosphate (NDP) using a spectrophotometer The measurement was done by determining the amount of ultraviolet (UV) light absorbed at a wavelength of 250 nm, which is the maximum absorbance point (λmax). Each result was calculated as the average of three measurements, with the standard deviation (SD) indicating the variability. The drug's efficacy percentage (EE%) was calculated using the following equation:

View Article Online
DOI: 10.1039/D4NA00510D

$$EE\% = \frac{Total\ amount\ of\ VLT - Unentraped\ VLT}{Total\ amount\ of\ VLT} X100$$

Determination of Particle size, PDI, and Zeta potential

Prior to measurements, each bilosomal formulation was diluted with deionised water to ensure the desired level of light scattering. The average values of PS (particle size), PDI (polydispersity index), and ZP (zeta potential) were determined using a Malvern Zetasizer Nano ZS instrument at a temperature of 25 °C. The PDI served as a measure of the uniformity of the size distribution. The ZP measurement was conducted by measuring the electrophoretic mobility of charged vesicles in an electric field [45].

The Creation of Gel Enriched with NDP Bilosomes

The optimised bilosomes, also known as NDP-Bilosomes, were incorporated with an appropriate gelling agent to enhance their retention on the epidermis for an extended period of time. The bilosomes gel, loaded with optimised NDP, was made using carbopol 940 (1% w/v) as a gelling agent. The carbopol 940, which had expanded overnight, was added to the NDP-Bilosomes dispersion and the NDP dispersion. The samples were stored overnight to allow the polymer to fully swell and gel [46]. To adjust the pH and keep them for subsequent examination, the gels were supplemented with triethanolamine (0.5%) and methylparaben (0.1%).

Gel Characterization

The viscosity of the gel that was created was assessed using a Brookfield viscometer. The study was conducted with the spindle C50-1 under ambient conditions. The pH of the bilosomal gel loaded with NDP was determined using a digital pH meter, while ensuring that the sample was appropriately diluted. The pH of the sample was determined by immersing the electrode for a duration of 2 minutes, followed by recording the corresponding pH value. The concentration of NDP in the gel was evaluated by dissolving 1 gramme of bilosomal gel loaded with NDP in 10 millilitres of methanol. The specimen was subjected to sonication in a bath sonicator and subsequently examined using a UV-spectrophotometer. The spreadability of the bilosomal gel loaded with NDP was assessed by applying it onto a sterile Petri plate and measuring its initial diameter. A second petriplate was positioned on top of the first petriplate, and a weight of 100 grammes was applied for a duration of 30 seconds [38]. The recorded value for the final dimension was used to determine the spreadability percentage using the provided equation:

View Article Online
DOI: 10.1039/D4NA00510D

$$\text{Spreadability (\%)} = \frac{Final\ diameter - intial\ diameter}{Intial\ diameter} X100$$

In Vitro Release Study

The release investigation was conducted by employing a pre-treated dialysis bag in a phosphate buffer solution containing ethanol in a ratio of 70:30 as the release medium, with a volume of 250 mL. The temperature was set at 32 ± 0.5 ◦C while maintaining a stirring speed of 50 rpm. The NDP-loaded bilosomal samples, NDP-loaded bilosomal gel samples, and drug solution samples (containing 2.5 mg of NDP) were placed into a dialysis bag and submerged in the release media. A sample of the released content (2 mL) was collected at specific time intervals (1, 2, 3, 4, 6, 9, 12, 24 h) and then replaced with fresh release media. The concentration was assessed using a UV spectrophotometer at a wavelength of 250 nm, with three measurements taken for each sample. The percentage of drug released over time was computed and a graph was created to show the relationship between the percentage of cumulative drug release and time. The release date of the NDP-loaded bilosomal gel was analysed using kinetic models, including the zero-order, first-order, Higuchi, and Korsmeyer-Peppas model. A graph was constructed and the R^2 value was computed to determine the most suitable kinetic release model.

Permeation Study

The permeation study utilised the egg membrane as it bears similarity to the stratum corneum of human skin [47, 48]. The eggs were obtained from the nearby chicken farm and immersed in a solution of hydrochloric acid that was diluted to a concentration of 0.1 N for a duration of 2 hours. The eggshell was chemically disintegrated, resulting in the separation of the membrane. The membrane was flushed with deionised water and subsequently dried at ambient temperature. The membrane was positioned between the donor and acceptor compartments of the diffusion cell, which had a volume of 20 mL and an area of 1.2 cm2. A solution consisting of phosphate buffer and ethanol (pH 6.8, 10 mL) was added to the acceptor compartment, with the stirring speed set at 50 rpm. The temperature was maintained at 32 ± 0.5 ◦C. The samples consisting of NDP-loaded bilosomal, NDP-loaded bilosomal gel, and medication solution (containing 2.5 mg NDP) were placed in the donor compartment. At specific time intervals (0.5, 1, 2, 3, 4, 6, and 12 hours), samples of 1 mL were taken from the receiving compartment and replaced with an equal volume of empty permeation media. The aliquots were passed through a membrane filter with a pore size of 0.25 µm, and the concentration was determined using a UV-vis spectrophotometer set at a

View Article Online
DOI: 10.1039/D4NA00510D

wavelength of 250 nm. The quantities of NDP that permeated, the rate of flux, the permeation coefficient (PC), and the enhancement ratio (ER) were computed [47,48].

$$\text{permeation coefficient} = \frac{Flux}{Area\ of\ Membrane\ X\ intial\ amount\ of\ VLT} X100$$

$$\text{ER} = \frac{PC\ of\ VLT{-}VLT\ loaded\ bilosomal\ gel}{PC\ of\ the\ conventional\ VLT\ gel} X100$$

Irritation Study

The irritability of the NDP loaded bilosomal gel was assessed by an in vitro HET-CAM assay, which serves as an alternative to the skin irritation test. The reason for using this test is that the blood vessel of the CAM has similarities to those found in humans and other animals utilised for testing [49]. The fertilised hen eggs were obtained from a nearby chicken farm and placed in an incubator for a period of 10 days. The incubator maintained a temperature of 37 ± 0.5 0C and a relative humidity of 60 ± 1%. On the tenth day, the egg was extracted from the incubator and the shell covering the air chamber was eliminated. The inner membrane, which was in direct touch with the CAM, became visible. The NaCl solution (0.9%) was applied to wet it, and the membrane was cautiously extracted using forceps. The NDP-loaded bilosomal gel, along with a positive control of sodium lauryl sulphate (1%w/v) and a negative control of 0.9% NaCl, were introduced to the CAM. The score was recorded at various time intervals, up to 5 minutes. The score was assigned based on a scale that ranged from no irritation (0–0.9), mild irritation (1–4.9, with minor decolorisation), moderate irritation (membrane decolorisation, 5–8.9), to complete haemorrhage (indicating severe irritation, 9–21) [49].

Solid state Characterizations

FTIR

The compatibility between NDP and bilosomal components was further examined using FTIR spectroscopy. The infrared spectra of pure NDP, CHL, and SDC, as well as the physical mixes of NDP with other bilosomal constituents previously described in the "DSC" section, were obtained using an IR spectrophotometer (Shimadzu 8400S, Lab Wrench, Japan). The samples were finely ground using 100 mg of dry potassium bromide powder, then compacted into transparent discs and scanned over the range of 400 to 4000/cm^{-1} [50].

Differential scanning calorimetry (DSC)

In order to examine the potential interaction between NDP and the components of vesicles, we conducted a thermal analysis using differential scanning calorimetry (DSC 60 Shimadzu, Japan). This analysis involved studying the thermal properties of pure NDP, CH, bile salt, a physical

View Article Online
DOI: 10.1039/D4NA00510D

mixture of NDP with bilosomal components, and the optimal bilosomes. The DSC instrument was calibrated using purified indium (99.9). The experiment involved mounting approximately 5 mg of each sample in standard aluminium pans. The samples were then heated in a temperature range of 10°C to 300°C at a scanning rate of 10°C per minute. The heating process was carried out under an inert nitrogen flow of 25 mL per minute [8].

Experiment using X-ray diffraction

An X-ray diffraction (XRD) investigation was performed on a specific bilosome containing NDP, as well as its related Bilosomal gel. The results were compared to those of the plain medication and the individual components, namely cholesterol and SDC. The chosen samples were prepared by subjecting them to irradiation with Cu Ka radiation filtered through Ni. The radiation was generated at a voltage of 45 kV and a current of 40 mA. In this work, the scanning rate was set at 2 scans per minute, covering a diffraction angle (2Θ) range of 3 to 70 [51].

Morphological Characterizations

The morphology and shape of Bilosomes was investigated by three techniques viz., SEM, TEM and AFM techniques. The SEM were performed to investigate the morphology of Bilosomes. They were coated with a layer of gold using a sputter-coating technique for SEM studies and were observed under low vacuum conditions with a magnification of 200. Similarly, TEM studies were performed to investigate the shape of Bilosomes. A small amount of the concentrated mixture was layered onto a copper grid that had been coated with carbon. The mixture was allowed to stick to the carbon surface for approximately 1 minute and then permitted to dry at room temperature for 10 minutes. Ultimately, the air-dried sample was seen at 20. Further, the prepared Bilosomes were also subjected to AFM studies to investigate the morphology further. A silicon cantilever shaped like a pyramid, which has a low-resonance frequency ranging from 250 to 331 kilohertz. This experiment produced intriguing findings, with a scanning rate of 0.5 Hz and a consistent force of 20–80 N/m exerted on the cantilever. After immersing mica in a solution containing newly formed vesicles for a whole day, observations were conducted [52–54].

***In-vivo* studies**

A total 57 Wistar rats were included in the in vivo investigations, specifically focussing on histopathological, skin deposition, and pharmacodynamic tests. Furthermore, a total of six male

View Article Online
DOI: 10.1039/D4NA00510D

Albino rabbits were included in the pharmacokinetic investigation. The Institutional Animal Ethics Committee granted consent for the investigation of pharmacokinetics and brain uptake (Protocol approval No. CPCSEA/IAEC/JLS/18/07/22/031). All investigations followed the EU directive 2010/63/EU in terms of using and managing animals. The animals were housed in cages with broad mesh wire bottoms to prevent coprophagy, while maintaining a temperature of 25°C and a humidity level of 55%. The animals were subjected to a 12-hour light-dark cycle and were given a regular food with unrestricted access to water. The animals had a 7-day period of acclimation prior to the commencement of the trials [55]. Drug-pools were created using lab-made containers that included a drug suspension and optimum Bilosomes for in-vivo investigations. The containers were placed on the previously depilated dorsal animal skin. Furthermore, the application was conducted in a non-occlusive manner within the drug reservoirs [38,56,57]. At the conclusion of the aforementioned investigations, animals were euthanised using the decapitation procedure after being administered anaesthesia.

In-vivo histopathological study

There were a total of nine rats, which were divided into three groups of three rats each. The therapy lasted for one day. Group I served as the control group, while group II and group III were administered a drug suspension and optimum bilosomes, respectively. The autopsy was conducted on skin samples, which were then preserved in a 10% solution of formaldehyde in saline for 24 hours. The samples were subsequently washed and dehydrated using alcohol. The specimens underwent xylene clearance and were then fixed in paraffin wax blocks. They were then sectioned at a thickness of 4 mm using a sledge microtome (Leica Microsystems SM2400). The samples were treated to remove paraffin, then stained and analysed using light microscopy (Axiostar plus, ZEISS, Oberkochen, Germany) for histological examination [58].

In-vivo skin deposition study

A total of twenty-four rats were divided into four groups, with each group consisting of six rats. Group I served as the control, while the animals in groups II, III, and IV were administered drug suspension, bilosomes, and ideal bilosomal gel, respectively. A fixed volume (0.5 mL) of drug suspension, bilosomes, and an optimised bilosomal gel were applied non-occlusively to a shaved section of the dorsal rat's skin. Following different treatment durations (1, 2, 4, 6, 8, and 10 hours), three rats from each group were euthanised and their dorsal skin was dissected and examined

View Article Online
DOI: 10.1039/D4NA00510D

[12,32,43]. The AUC0–10 values were computed and compared among the different treatments. The study examined statistical significance by utilising one-way ANOVA with SPSS® software version 22.0. A post-hoc test was performed using Tukey's HSD test.

In-vivo pharmacodynamic study

A pharmacodynamic investigation was conducted using a noninvasive blood pressure arrangement (NIBP 200 A; Biopac System, Inc., Goleta, CA, USA) based on the tail cuff method. A total of twenty-four Wistar rats were evenly divided into four groups, labelled 1 to 4. Group 1 functioned as the standard control group. Hypertension was induced in the other groups (2, 3, and 4) with subcutaneous administration of methylprednisolone acetate for a duration of 2 weeks. Group 2 served as the control group for hypertension. Group 3 was given crushed oral tablets (40 mg NDP) (Diovan® 40 mg oral tablets) using an oral gavage syringe for administration. Group 4 was administered a topical therapy of an optimum bilosomal gel containing 10 mg of NDP. The NDP bilosomes dispersion was applied topically to a shaved dorsal region of the rat's skin, covering an area of 4.91 cm2. The tail blood pressure (BP) was subsequently measured at predetermined time intervals. The statistical analysis was conducted using one-way ANOVA using SPSS® software version 22.0. A posthoc test was conducted using Tukey's honestly significant difference (HSD) test. The percentage drop in blood pressure from the hypertensive control was calculated [59].

In-vivo pharmacokinetic study

Animal study protocol

The in-vivo pharmacokinetic investigation utilised six male Albino rabbits. Animals were categorised into two categories of equal size. A randomised crossover design was conducted, consisting of two stages with a washout time of 1 week between them. The hair on the upper side of the initial group was removed, and a specific area measuring 10 cm×5 cm was treated with an ideal dose of 40 mg NDP laden bilosomes. In addition, the second group received oral NDP tablets with a dosage of 40 mg (specifically Diovan® 40 mg oral tablets) administered orally using oral gavage. After the time of heavy rain, the randomisation process was reversed. Two millilitre blood samples were collected by puncturing the retro-orbital plexus using heparin-coated eppendorf tubes at various time intervals: 0, 1, 2, 3, 4, 6, 8, and 12 hours after injection. The plasma was subjected to centrifugation at a speed of 5000 revolutions per minute for a duration of 15 minutes. Subsequently, it was stored at a temperature of -20°C until it was ready for analysis [60].

View Article Online
DOI: 10.1039/D4NA00510D

Monitoring of drug distribution

The presence of nimodipine, the active form of NDP, was detected in plasma samples using a highly sensitive, accurate, and specific liquid chromatography mass spectrometry (LC/MS/MS) method. The NDP concentration was graphed with time and analysed using non-compartmental models with Kinetica® 5 software from Thermo Fisher scientific Inc., Waltham, MA, USA. The maximum concentration (Cmax) and time to reach maximum concentration (Tmax) were calculated. Furthermore, the values for AUC0–48 and AUC0–∞ were computed. The Cmax, AUC0–48, and AUC0–∞ values were compared between the treatments using an analysis of variance (ANOVA) test with the SPSS® software version[61], The nonparametric Signed Rank Test, also known as Mann-Whitney's U test, was employed to compare the medians of Tmax for the different treatments. The relative bioavailability of optimum bilosomes was determined and compared to the oral tablets using the following equation [62]:

$$\text{Relative bioavailability} = \frac{\text{AUC NDP bilosomes}}{\text{AUC oral tablets}} X100$$

Stability Studies for NDP-Loaded Bilosomes

The stability of the optimised bilosomes preparation, loaded with NDP, was assessed by storing them in glass vials at a temperature of 4 ± 1◦C for a duration of three months. The physical stability was assessed by comparing the particle size and EE data before and after storage [63].

Statistical analysis

The data were presented as the mean value plus or minus the standard deviation (SD). The statistical analysis of the mean difference between groups was conducted using one-way ANOVA, followed by Tukey post hoc analysis. The significance level was established at a p-value of less than 0.05. The computations were performed using the computer software SPSS 22 (SPSS, Chicago, IL).

Results and Discussions

Analyzing in a combinatorial approach

A full factorial design is an advantageous method for investigating the combined impact of formulation factors on the features of vesicles, while minimising the number of experiments required. This design allows for the simultaneous variation of all selected formulation factors, while also analysing their effects and any potential interactions on the measured responses. This

View Article Online
DOI: 10.1039/D4NA00510D

eliminates the need for conducting separate independent investigations. A 33 complete factorial design was employed and subsequently subjected to statistical analysis using Design-Expert® software. The levels of each ingredient were determined based on early studies and the practicality of manufacturing NDP loaded bilosomes at these values. The chosen model was a two-factor interaction (2 FI) model. The signal-to-noise ratio was assessed to ensure the model's precision is sufficient for navigation purposes [64]. All responses in Table 3 exhibited a ratio that exceeded 4, which is considered desirable. Moreover, the R-squared statistic was computed to assess the model's ability to accurately fit new data that follows the same connection as the one modelled. The adjusted R-squared statistic is a revised version of the R-squared statistic that quantifies the extent to which the model will accurately fit the observed data. Therefore, it is desirable for the adjusted and anticipated R2 values to be similar [65]. Upon examining the design analysis results (Table 3), it was observed that the projected R2 values were reasonably consistent with the adjusted R2 values for all replies. The projected R2 score of PDI suggests that the average value is a more effective indicator of the outcome [61]. This could be attributed to the fact that the PDI of the manufactured bilosomes was not influenced by the conditions under investigation. The utilisation of a full factorial design in this study is the optimal choice for an experimental design. This is due to its inclusion of all potential combinations of the variables under investigation, at the designated levels. Consequently, this design effectively reduces any uncertainty or ambiguity. Each combination can be assessed for a variety of distinct qualities, known as responses. Table 2 presents the EE numbers, vesicle size, and the percentage of medication released for all 27 combinations of the 3^3 complete factorial design[66].

Table 2. The experimental parameters, independent factors, and measured responses of 3^3 combinatorial layouts of NDP-loaded bilosomes

Run	Type of surfactant	Surfactant: Cholesterol	SDC	Y1: %EE	Y2: Particale size	Y3: PDI	Y4: Zeta potential
1	Span 20	1:1	5	45.37±0.56	285.31±5.36	0.456±0.02	-39.61±1.23
2	Span 60	1:1	10	60.59±0.96	185.34±12.5	0.238±0.01	-40.21±0.96
3	Span 20	1:1	10	57.62±1.24	205.34±8.94	0.361±0.05	-36.28±2.15
4	Span 60	8:2	20	88.56±1.73	165.38±2.64	0.195±0.13	-25.97±2.11
5	Span 60	1:1	5	53.64±0.94	254.13±10.5	0.243±0.02	-41.03±0.98

View Article Online
DOI: 10.1039/D4NA00510D

6	Span 40	8:2	10	68.51±1.05	213.54±6.58	0.157±0.05	-24.31±2.31
7	Span 60	2:8	5	64.25±0.34	196.35±7.32	0.291±0.04	-38.49±0.46
8	Span 20	8:2	20	70.83±1.06	145.89±9.54	0.243±0.01	-23.46±1.28
9	Span 60	8:2	10	75.41±2.01	156.3210.2	0.269±0.03	-26.49±0.67
10	Span 20	2:8	20	69.34±1.35	234.51±15.6	0.138±0.05	-29.64±1.35
11	Span 20	1:1	20	63.84±0.64	256.94±11.4	0.386±0.04	-33.21±2.04
12	Span 40	8:2	5	76.54±0.59	189.36±13.8	0.149±0.12	-25.73±1.54
13	Span 40	2:8	10	59.84±1.25	203.59±8.92	0.342±0.01	-36.49±0.96
14	Span 20	2:8	10	58.73±0.43	249.73±6.53	0.296±0.03	-42.01±0.52
15	Span 60	2:8	20	79.61±0.38	204.31±9.42	0.264±0.05	-32.19±1.82
16	Span 40	1:1	5	65.21±0.68	213.05±11.2	0.217±0.04	-29.84±0.59
17	Span 40	2:8	20	76.39±1.22	154.09±13.5	0.169±0.01	-22.06±1.03
18	Span 60	8:2	5	73.05±0.69	168.42±18.4	0.304±0.06	-41.05±2.54
19	Span 20	2:8	5	48.92±0.53	256.37±12.4	0.186±0.05	-36.54±1.67
20	Span 20	8:2	5	52.76±1.27	201.46±10.5	0.385±0.02	-36.59±2.93
21	Span 60	2:8	10	76.82±0.34	169.53±11.6	0.432±0.03	-40.37±0.59
22	Span 40	1:1	20	70.53±1.20	175.28±14.2	0.208±0.01	-32.85±1.05
23	Span 40	2:8	5	63.09±0.69	199.32±13.4	0.185±0.12	-20.41±2.11
24	Span 40	1:1	10	60.95±0.12	196.83±5.49	0.167±0.01	-48.37±0.49
25	Span 40	8:2	20	75.64±1.32	136.48±7.82	0.149±0.11	-24.31±1.03
26	Span 20	8:2	10	60.37±0.28	186.35±6.49	0.318±0.01	-21.04±0.54
27	Span 60	1:1	20	69.28±1.04	289.37±5.31	0.159±0.12	-29.68±0.32

Effect of Formulation Variables on the EE% (Y1) of NDP -Loaded Bilosomes

Effect of surfactant type

In general, bilosomes made with span 60 showed better EE compared to those prepared with other spans. This can be due to the effects of the length of the alkyl chain on the vesicles. Span 60, with its longest saturated alkyl chain (C18), produces membrane bilayers that are more stable compared to span 40 (C16) and span 20 (C12). Additionally, the length of the alkyl chain has an impact on the hydrophilic-lipophilic balance (HLB) value of the surfactant, which can subsequently affect the efficiency of drug entrapment. Specifically, a lower HLB value in the surfactant will result in

View Article Online
DOI: 10.1039/D4NA00510D

a higher drug EE. The literature has shown this phenomenon in niosomes that were manufactured using span 60 (HLB=4.7) and span 20 (HLB=8.6). The latter resulted in a decreased EE. According to the published data, the EE improves in the order of sp20< sp40< sp60, which was also corroborated by our findings.

Effect of surfactant (SAA): Cholesterol (CH) ratio on EE %

The proportion of SAA (Surface Active Agent) to CH (Cholesterol) is crucial in influencing the characteristics and behavior of the bilayer in the produced vesicles [67]. The data obtained indicated that increasing the ratio of CH relative to SAA from 8:2 to 1:1 resulted in an increase in EE percentage, except in the case of span 20 where the 8:2 ratio exhibited a greater EE percentage compared to the 1:1 ratio. The inclusion of additional CH, in a 2:8 ratio, resulted in the lowest EE% regardless of the surfactant type utilized, while maintaining the same SDC quantity. The observed outcomes can be attributed to the stiffness and thickness added to the bilayers when cholesterol is introduced, resulting in the formation of highly organized vesicles [68]. By stabilizing the bilayer membrane and reducing drug leakage from the aqueous core structures, this can improve the entrapment efficiency of hydrophilic medicines[20]. Upon further addition of cholesterol, a notable reduction in EE % was found ($p<0.05$). This drop may be attributed to the rivalry between cholesterol and the drug for the available space inside the bilayer structure, leading to disruption and subsequent leakage of the drug[69,70]. Abdelbary et al. observed that as the cholesterol ratio increases beyond a certain limit, there is a fall in EE %, perhaps because high concentrations of cholesterol can alter the normal structure of vesicles[71,72].

Effect of SDC on EE %

The results demonstrated a positive correlation between the amount of SDC and the rise in EE%. This can be attributed to the anionic properties of SDC, which induce a negative charge on the vesicles. Consequently, this generates a strong repulsive force between the lamellae. Consequently, the interior aqueous core expands in size, resulting in an elevated encapsulation efficiency (EE) of the lipophilic drug NDP. This finding was also seen by Noha S. El-Salamouni et al., who achieved comparable outcomes [21,73].

Analysis of factorial design

View Article Online
DOI: 10.1039/D4NA00510D

In order to create a strong bilosomal formulation, it is crucial to determine if the impact of the formulation variables and/or their interactions on the observed outcomes is statistically significant. Moreover, understanding the size and direction (positive or negative) of the impacts (referred to as estimations) can assist in optimizing the bilosomal formula. Statistical analysis of the impact of the formulation variables on the efficiency percentage of EE:To determine the effects, the experimental EE values were fitted to a standard least square model. The results demonstrated a strong connection, shown by a p-value of less than .0001 and an R-squared value of 0.9230. The table 2 displays the estimated impact of the independent variables on EE [74].

Table 2 reveals that the impacts of individual components, X1, X2, and X3, are statistically significant with a p-value of less than 0.05. The estimation of the impact of SAA exhibits a negative sign for span 20, indicating a considerable decrease in EE when this surfactant was employed. Substituting span 20 with span 60 resulted in a significant and noticeable improvement, as evidenced by the increase in EE% when this particular form of SAA was employed. The SAA: CH ratio of 1:1 yielded favorable results when span 60 was employed. However, when span 20 was utilized, it had a detrimental impact. Nevertheless, the effect shifted to positive with a lower cholesterol level of 8:2. A strong positive estimate for SDC on the EE indicates that an increase in this component results in a significant rise in EE. Table 2 shows that the interaction of X1*X2 is statistically significant ($p<0.05$). This is visually represented in figure 1, where the intersecting interaction plots and the lack of parallelism in the lines indicate a significant interaction effect between X1 and X2 at various levels of X3. However, the interactions between X1 and X3, as well as between X2 and X3, did not show statistical significance ($p>0.05$)[75].

The Model F-value of 18.30 indicates that the model is statistically significant. The probability of an F-value of this magnitude occurring solely due to noise is only 0.01%. P-values below 0.0500 imply that the model terms are statistically significant. The significant model terms in this example are A, B, C, AB, and AC. The Predicted R^2 value of 0.7300 is reasonably close to the Adjusted R^2 value of 0.9230, with a difference of less than 0.2. Adeq Precision quantifies the ratio of signal to noise. A ratio over 4 is preferable. The ratio of 17.274 suggests that the signal is sufficient. This paradigm is applicable for navigating the design space. The size of the particles loaded with NDP in bilosomes ranged from 136.48±7.82nm (NDP -B 25) to 289.37±5.31nm (NDP -B 27). The polydispersity index (PDI), which indicates the breadth of the size distribution of the particles,

View Article Online
DOI: 10.1039/D4NA00510D

varied from 0.138±0.05 to 0.456±0.02. The low PDI values suggest the presence of a population of vesicles that are uniform in size and composition[76].

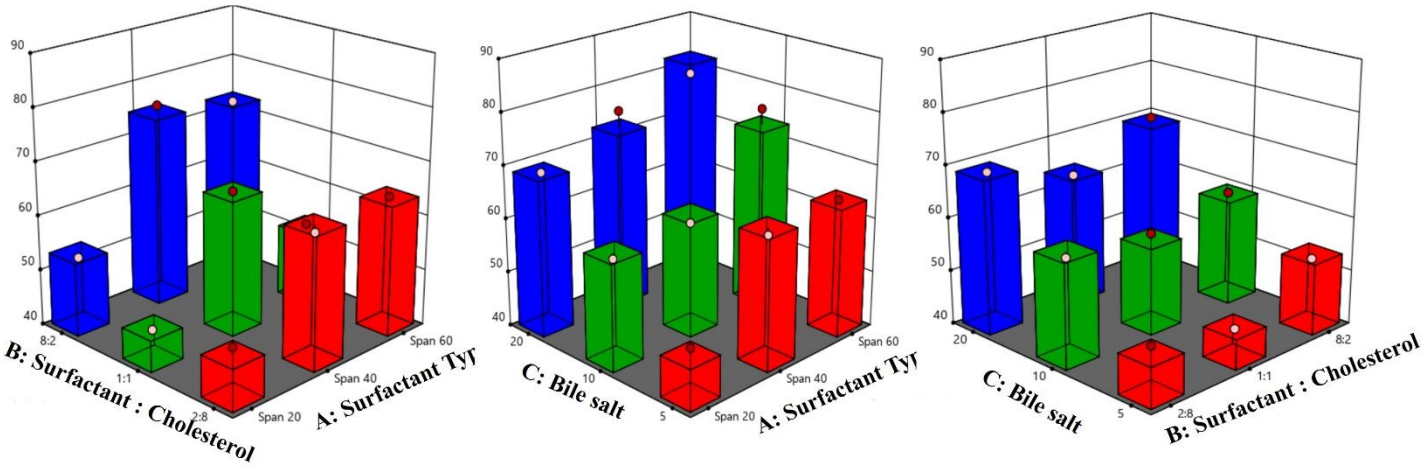

Figure 1. Effect of Formulation Variables on the EE (Y1) of NDP-Loaded Bilosomes

Effect of surfactant type on particle size

Table 2 demonstrates that the bilosomes based on span 20 have a higher vesicle size in comparison to those based on span 40 and span 60. This can be attributed to the reduction in surface energy caused by the presence of hydrophobic surface-active agents (SAA) with reduced hydrophilic-lipophilic balance (HLB), resulting in a smaller particle size [77,78]. According to the data in table 2, the particle size of all bilosomes based on span 40 and span 60 is below 200 nm, which is considerably lower than the particle size of bilosomes based on span 20 ($p<0.05$). The results are consistent with the findings of Yusuf et al., who observed that employing a surfactant with a lower hydrophilic-lipophilic balance (HLB) led to the formation of vesicles with reduced size[79]. Additionally, Abdelbary & Aburahma observed that the water absorption of SAA increases as the HLB values shift towards the hydrophilic area, leading to an enlargement in the size of vesicles [80].

Effect of SAA: CH ratio on particle size

View Article Online
DOI: 10.1039/D4NA00510D

The impact of the SAA: CH ratio on the size of NDP-loaded bilosomes vesicles increased in the following sequence: 8:2>1:1>2:8. This tendency was confirmed under all formulation conditions, regardless of the type or quantity of surfactant utilized. The results demonstrated that an increase in cholesterol ratio led to an enlargement in vesicle size. This might be attributed to the disruption caused in the vesicular membrane by heightened hydrophobicity, resulting in the formation of larger vesicles [81].

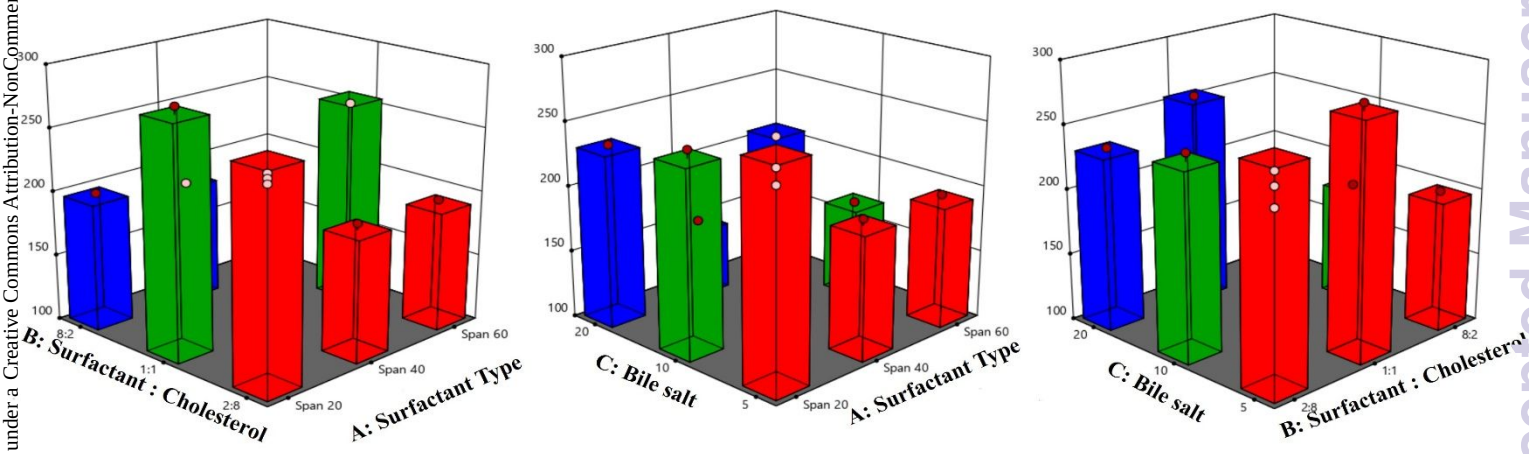

Figure 2. Effect of Formulation Variables on the Particle size (Y2) of NDP -Loaded Bilosomes

Effect of SDC on particle size

The results indicated that increasing the amount of SDC from 5 mg to 10 mg and up to 20 mg resulted in a bigger size of vesicles. The larger size of the vesicles can be explained by the strong repulsive attraction generated by the negatively charged nature of SDC, which leads to an expansion of the interior aqueous core space[82]. Statistical analysis of the impact of the formulation variables on particle size: The table 2 displays the estimations of the impact that the independent factors have on the particle. Statistical analysis reveals that all single factors, X1, X2, and X3, except for X2 at a 1:1 ratio, have significant effects ($p<0.05$). The assessment of the impact of SAA reveals a favorable outcome for span 20, but a negative outcome for span 40 and span 60. This indicates that the particle size rose with span 20, but decreased at the other levels of this component. The estimated effect of SDC is positively correlated with a value of 26.76, indicating that higher SDC concentrations lead to an increase in the particle size of the bilosomes. The estimation of the impact of the ratio indicates a negative value at a 2:8 ratio (at elevated cholesterol levels), suggesting that an increase in the cholesterol ratio results in a reduction in particle size. Nevertheless, the result is positive for the remaining levels of the ratio. The impact of the

View Article Online
DOI: 10.1039/D4NA00510D

interaction is statistically insignificant ($p>0.05$), as supported by the parallel lines observed in figure 2. The mathematical model that describes the VS can be utilized to forecast the values by integrating the statistically meaningful estimations of the impacts of a single factor. When SAA is mixed with CH at a ratio of 1:1, it results in the formation of span 60.

Particle size = +203.43 -16.59 +25.64 +14.77

Impact of manufacturing parameters on PDI of bilosomes loaded with NDP

The polydispersity index (PDI) of NDP loaded bilosomes ranged from 0.138±0.05 to 0.456±0.02, as shown in Table 2. The impact of the type of surfactant (X1), the ratio of surfactant to cholesterol (X2), and the quantity of bile salt (X3) on the polydispersity index (PDI) of bilosomes loaded with NDP is visually represented in Figure 3 through 3-D graphs. The ANOVA analysis showed that the PDI of the produced vesicles was not substantially influenced by any of the conditions under investigation.

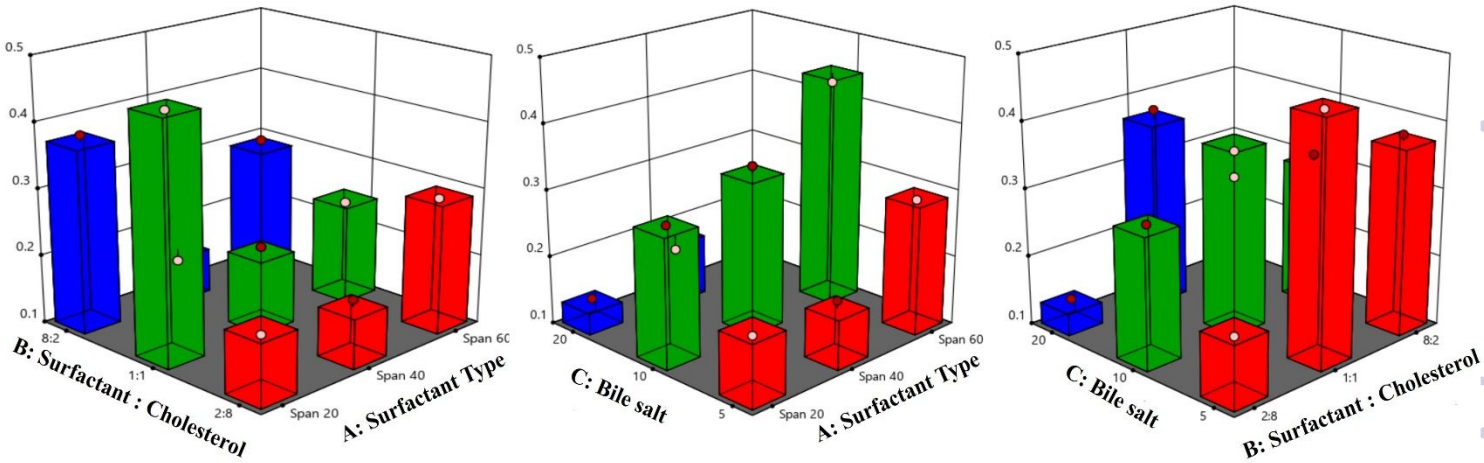

Figure 3. Y3 Poly Dispersity Index of NDP-Loaded Bilosomes as the Function of Formulation Variables

Zeta potential of NDP-loaded bilosomes as a function of manufacturing parameters

View Article Online
DOI: 10.1039/D4NA00510D

All NDP loaded bilosomes exhibited negative zeta potential (ZP) values, ranging from -20.41±2.11 to -42.01±0.52 mV (Table 2). Therefore, the NDP vesicles possessed an ample amount of charges that protected them against both aggregation and fusion[83]. Given that all formulations yielded negative ZP values, it is necessary to utilize the absolute values for discussion in order to avoid any potential misinterpretation. The impact of surfactant type (X1), SAA:CH ratio (X2), and bile salt quantity (X3) on the zeta potential (ZP) of NDP loaded bilosomes is visually represented as 3-D plots in Figure 4. According to the analyzed design, only the type of SAA (X1) and the amount of bile salt (X3) had a significant impact on the ZP values of the generated bilosomes (P = 0.0028 and P = 0.0090, respectively). Regarding the specific SAA (X1), it was demonstrated that span 60 had a greater affinity for the vesicular lipid bilayer compared to span 40 and span 20 in the produced vesicles, resulting in a higher charge. The greater ZP values of vesicles made with span 40 compared to those prepared with span 20 can be attributed to the fact that the span 20 conjugation has a larger hydrophilic-lipophilic balance (HLB) than the unconjugated homologues, resulting in a higher charge intensity of the vesicles [84]. It is worth noting that Span 20 has a higher HLB value than Span 60. Nevertheless, Span 20 exhibited greater ZP values on the vesicular bilayer in comparison to Span 60. The increased ionization of span 20 compared to span 40 can be attributable to its stronger hydrophilic-lipophilic balance (HLB) value. Bile salts act as electrostatic stabilizers by increasing the surface charge density of vesicles, hence enhancing their stability. Nevertheless, augmenting the quantity of bile salt (X3) markedly reduced ZP levels. The observed

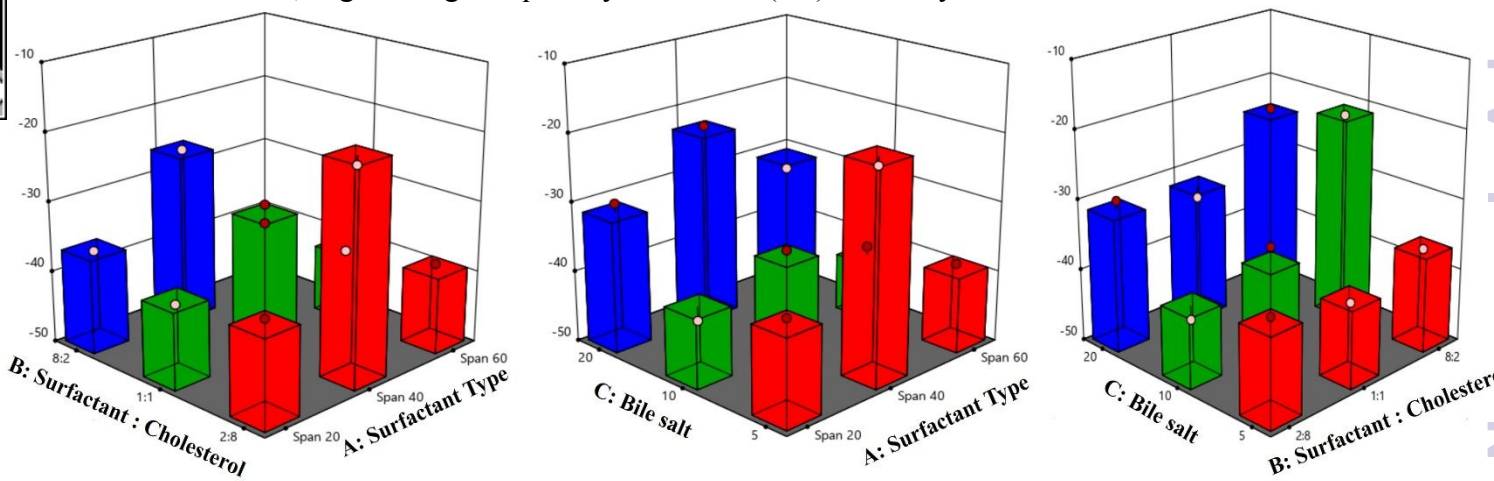

Figure 4. Effect of the zeta potential (Y3) of NDP-loaded bilosomes as a Function of Formulation Variables

View Article Online
DOI: 10.1039/D4NA00510D

phenomenon can be explained by the fact that when the amount of bile salt exceeds a particular threshold, it disrupts the electrostatic double layer, leading to a considerable fall in Zeta Potential (ZP) [85].

Selection of the Optimized Bilosomal Formulation

Numerical optimization with the desirability technique yields the best physicochemical attributes and an efficient, high-quality outcome. Ideal transdermal delivery systems meet these criteria: Vesicles no larger than 200 nm with high release efficiency should fit in the skin's intercellular lipid domains to deliver a constant dose of medicine. We found the ideal variable settings by applying Table 1's limits to the Design Expert's desirability function. These restrictions included the zeta potential (Y4), PDI range (Y3), lowest VS (Y2), and maximum EE% (Y1). Figure 5 shows the three-dimensional surface plots for Y1, Y2, Y3, and Y4 created with Design Expert®. The top three bilosomes were F4, F15, and F24. This led to their selection for extra-ex vivo research.

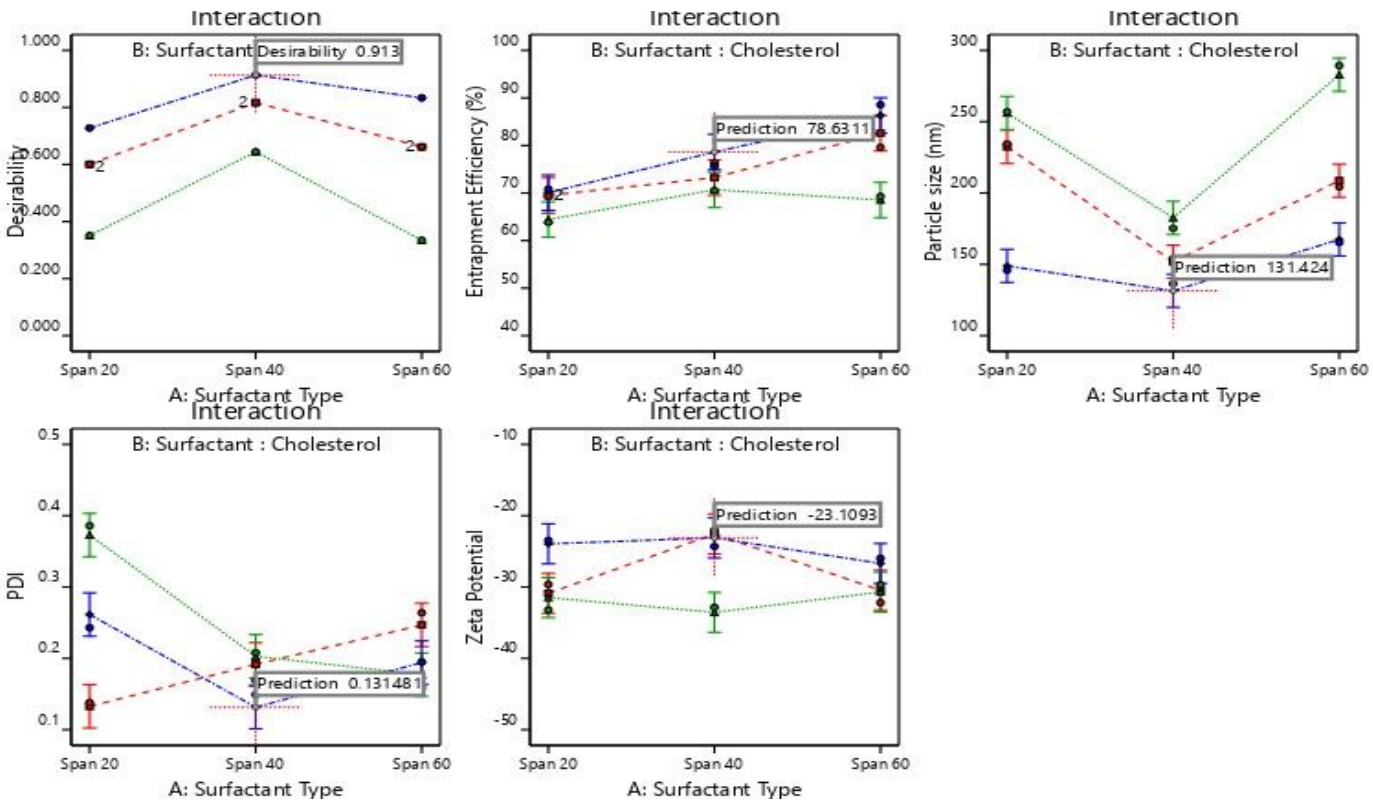

Figure 5. Interaction between the dependent and independent variables of NDP-loaded bilosomes

View Article Online
DOI: 10.1039/D4NA00510D

Development of NDP-loaded bilosomal gel

Next, add 1% Carbopol 940 gelling agent to the NDP-loaded bilosomal gel. We determined the gel properties by testing 0.75%, 1%, and 1.25% carbopol. The gel with 1% carbopol w/v had ideal spreading, viscousness, and extrudity. Therefore, we used optimized NDP bilosomes with a surfactant type span of 60, SDC (30 mg), and an 8:2 SAA: CH ratio to create a transdermal gel with 1% carbopol.

Viscosity, pH, and Drug Content

We measured the drug content, pH, and viscosity of NDP-loaded bilosomal gel. The formulation had a viscosity of 1356 ± 15.6 cps, indicating good skin retention. Similar to the skin pH, the pH was measured at 6.82 ± 0.2. The NDP-loaded bilosomal gel exhibits a drug concentration of 99.68 ± 1.53%. The uniform distribution of NDP throughout the gel allows for identifying the most likely drug. The spreadability rating in square inches was crucial for applying gel to the skin. Results indicate an excellent spreading capacity, with an area of 6.02 ± 0.51 cm^2.

***In Vitro* Release Study**

In *vitro*, drug release testing enhances *in vivo* behavior. This method measures drug absorption and bilosomal vesicles' effect on drug penetration. Biosome vesicles trap drug molecules in the aqueous medium. The dialysis bag membrane controlled drug diffusion into the receptor medium. We studied the release behaviour of NDP-bilosomes, NDP-bilosomal gel, and pure NDP solution. The results are visualized in Figure 6. The highest NDP release in 24 hours was seen in NDP-bilosomes (90.26 ± 2.38%), NDP-Bilosomal gel (68.79 ± 1.29%), and pure NDP solution (96.37 ± 1.04%). Three hours saw the complete release of pure NDP. The encapsulation of NDP in two nano-sized bilosomes resulted in a high release, while surfactants enhanced the drug's penetration. The tiny particle's increased effective surface area enhances absorption. Surfactant and bile salt decreased the surface interfacial tension, which made it easier for NDP to dissolve and mix with discharge fluids. The BS's surface facilitated the quick release of NDP for three hours, while the slow diffusion of the lipid matrix ensured a constant release. The new NDP-loaded bilosomal gel released NDP more slowly than NDP-bilosomes. A carbopol matrix added a barrier, slowing medication release. Particles must cross both layers to reach the release medium [86]. Delaying drug release maximizes absorption. Due to its slow and sustained release, NDP-loaded bilosomal gel is appropriate for transdermal administration since it maintains therapeutic effectiveness after a quick

View Article Online
DOI: 10.1039/D4NA00510D

release. The Korsmeyer-Peppas model was the best-fitted release kinetics model, with a maximum regression value of R2 = 0.9539. The release exponent n = 0.45 (range: 0.43 to 0.85), which suggests anomalous transport, raised the possibility.

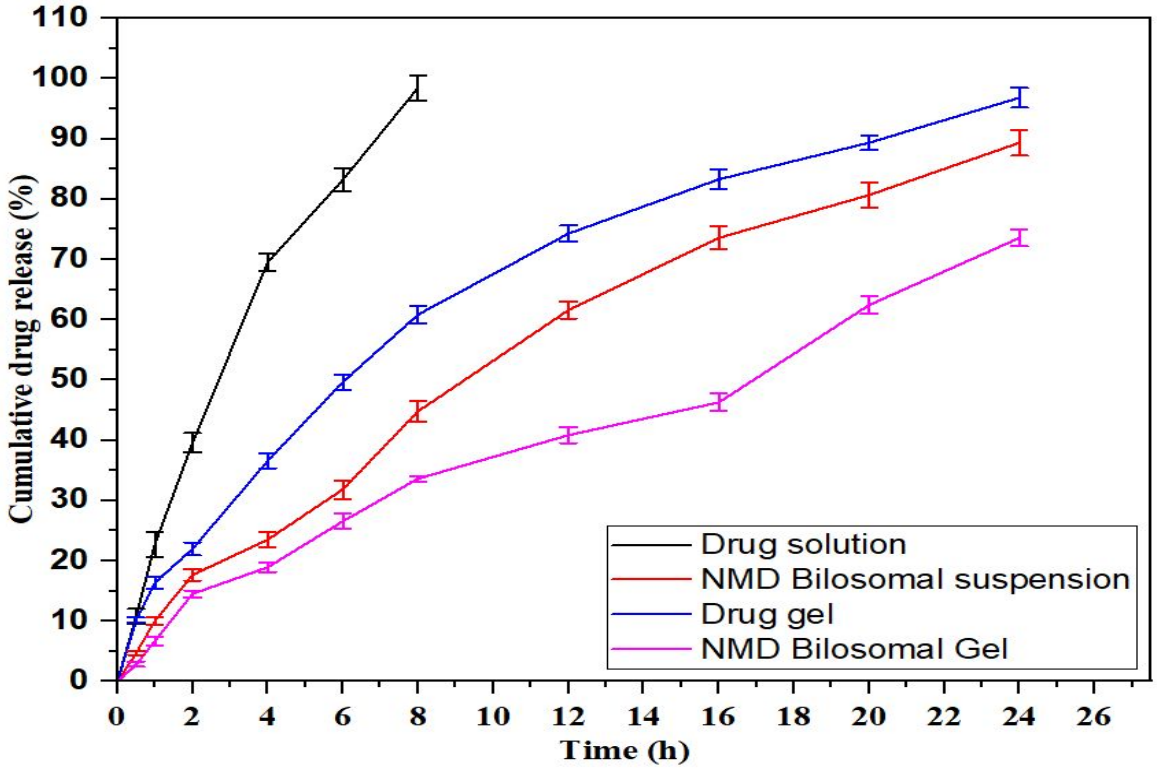

Figure 6. NDP-bilosomes, NDP-Bilosomal gel, pure drug gel, and pure NDP solution *in-vitro* release of NDP.

Permeation Research *In Vitro*

Figure 7 predicts egg membrane permeability to NDP-bilosomes, NDP-bilosomal gel, and pure NDP solution. The rate of NDP permeation was 63.28 ± 1.3% with NDP bilosomes, 45.37 ± 0.67% with NDP-Bilosomal Gel, and 18.07 ± 1.35% with pure NDP. The previously generated formulas could also determine the flow. The NDP-Bilosomal gel had a substantially lower flow rate (12.38 µg/h/cm2) compared to NDP-bilosomes (18.29 µg/h/cm2), with a p-value < 0.05. Surfactant reduces viscosity and accelerates NDP release, resulting in a faster release rate than untreated ones. Surfactant and bile salt permeability relax the cell membrane's tight junction, boosting medication potency. The low flow rate of 3.26 µg/h/cm2 in pure NDP was due to its low solubility and permeability. Results show APC values of 12.37 × 10−3, 7.02 × 10−3, and 2.86 × 10−3 for NDP-bilosomes, NDP-bilosomal gel, and pure NDP. The enhancement ratio showed that NDP-

View Article Online
DOI: 10.1039/D4NA00510D

bilosomes increased 1.76-fold, whereas NDP-bilosomal gel and pure NDP dispersion increased 2.45-fold. The flow of NDP-Bilosomal gel was 1.39 times that of pure NDP dispersion.

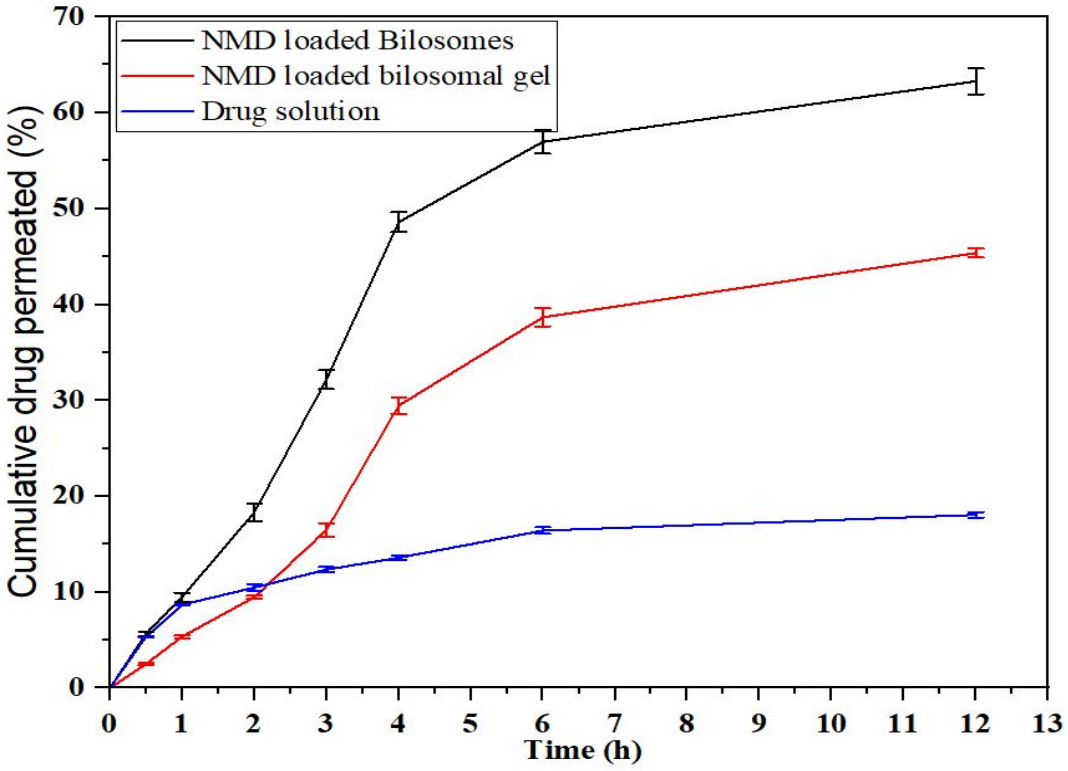

Figure 7. Egg membrane permeability of NDP bilosomes, gel, and pure NDP. The research was done in triplicate and presented as mean ± SD.

Irritation Study

The HET-CAM test measured the irritation of the negative control (0.9% w/v NaCl), positive control (1% w/v sodium lauryl sulphate), and NDP bilosomes gel. The mean annoyance score and treatment group scores were monitored. The negative control sample was never uncomfortable (0-0.9), whereas the positive sample scored very high (17.44). A 9-21 score indicates an irritating sample. The created NDP bilosomes gel scored 0, indicating no CAM irritation. We know the negative control and produced formulation will not irritate the skin because they have zero membrane irritation ratings.

Solid state characterization

The FTIR system

View Article Online
DOI: 10.1039/D4NA00510D

Nimodipine and the excipients employed FTIR to determine molecular interactions and changes. The addition of new peaks, alteration of the diameter of the current peak, or elimination altogether indicates molecular interactions. Nimodipine and its excipients used FTIR to determine molecular interactions and changes. Adding peaks, changing peak diameters, or eliminating peaks suggest molecular interactions. Physical interaction, Nimodipine, NDP-bilosomes, and gel formation Fourier transform infrared spectra are shown in Figure 8. Studying the FTIR spectrum of pure NDP showed that it had aliphatic C-H stretching vibrations, carboxylic-COOH, amidic, aromatic C=C, and C-O at 2952, 2869, 1722, 1593, 1460, 1268, and 756 cm^{-1}. Infrared spectra of SDC showed a broad absorption peak at 3390.86 cm^{-1}, indicating hydroxyl group stretching (Fig. 2B). Later investigation indicated vibrational peaks at 2938.10, 2862.36, 1558.48, and 1064 cm^{-1} for COO− and C-O, respectively. Three distinct peaks at 3429.43 cm^{-1}, 2920.23 cm^{-1}, and 1716.65 cm−1 in Span 60 spectra revealed the -OH, -COOH, and -CHO functional groups. In the CHL spectra, the hydroxyl functional group occurred at 3417.86 cm1 and the carboxylic acid functional group at 2929 cm^{-1}. Figure 8 displays the enhanced FTIR spectra of NDP-loaded bilosomes, with numerous bands appearing larger due to lower DSC crystallinity. The spectra showed no significant band changes. The alterations in bilosome vesicles indicated Nimodipine's existence.

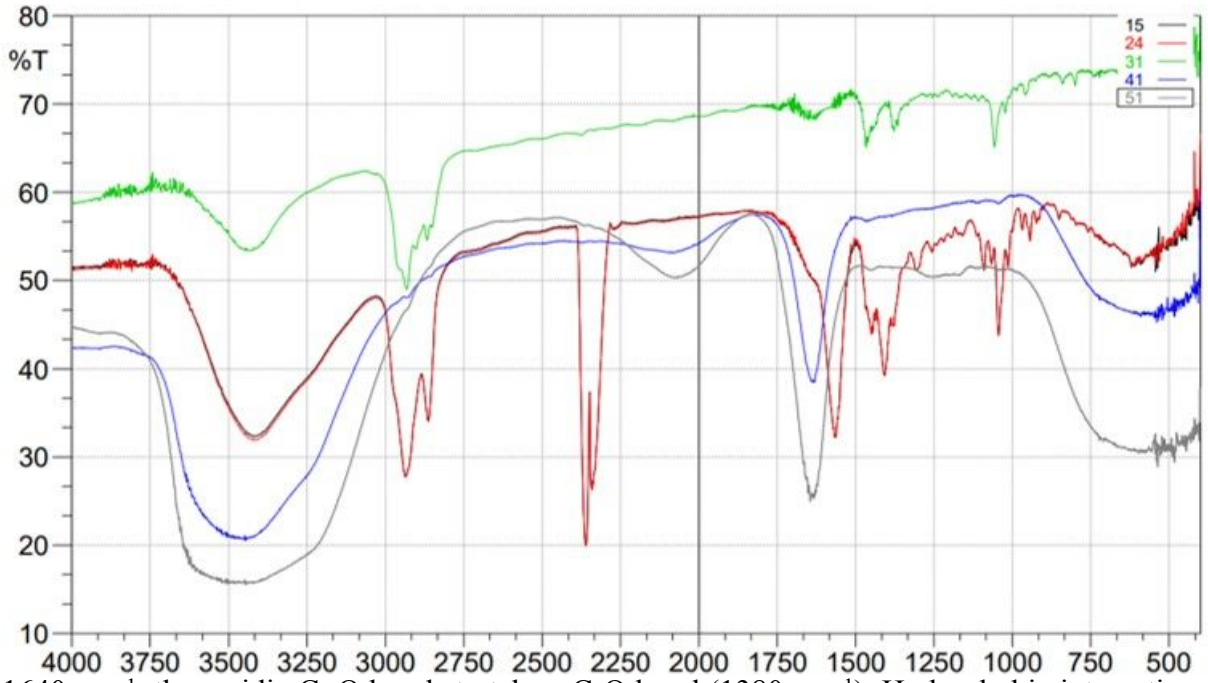

At 1640 cm^{-1}, the amidic C=O bond stretches. C-O bond (1380 cm^{-1}). Hydrophobic interactions between nimodipine and bilosomes help generate stable, optimal vesicles.

View Article Online
DOI: 10.1039/D4NA00510D

Figure 8. FTIR analysis of Nimodipine (NMD), Sodium deoxycholate (SDC), NMD-loaded biolosomes, NMD-loaded biolosomes gels

Differential Scanning Calorimetry (DSC)

The DSC instrument identified the optimal formulation (NDP-bilosomes and bilosomal gel), the physical mixture (Nimodipine and SDC), and the thermal behaviour and interactions of the drug. In the DSC experiments, we observed endothermic peaks in the drug, physical mixes (drug and SDC), optimized NDP-bilosomes, and bilosomal gel, as illustrated in Figure 9. The drug's crystal structure changed when endothermic or exothermic peaks disappeared or altered. DSC thermogram analysis revealed an endothermic peak at 103.51 °C and an enthalpy of −42.60 J/g for Nimodipine. The material was pure crystal due to the significant endothermic peak. At 188.24 degrees Celsius, thermogravimetric analysis of solids (SDC) showed endothermic peaks. The physical combination of these substances lowered the pharmacological peak. Bile salt and cholesterol components melting and interacting with Nimodipine could have been the cause of this. It was likely possible that the hydrophilic drug could have been partially incorporated into the melted lipid. Kumari and Pathak, and Shaji and Lal had similar findings. SDC endotherms were 62.31 °C, and cholesterol endotherms were 148.84 °C in optimized Nimodipine bilosomes and bilosomal gel, respectively. As illustrated in Figure 9, the optimized formulation produced a less crystalline medicament with a higher peak than the melting point. Displays an optimized composition compared to other excipients that did not interact with NDP-loaded bilosomes. Nimodipine's melting endotherm absence suggests an amorphous complex. Nidipine's effects on bile salts may

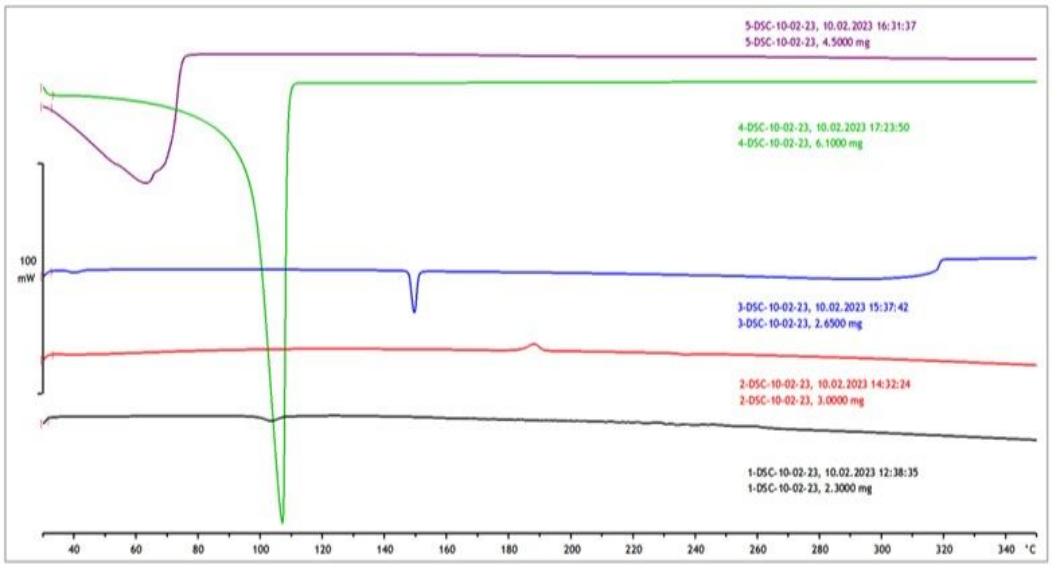

View Article Online
DOI: 10.1039/D4NA00510D

explain its better drug retention in bilosomes. DSC and FTIR showed that nimodipine strongly interacted with bilosomal components. Hathout and Mohamed's proof.

Figure 9. DSC studies Nimodipine (NMD), Sodium deoxycholate (SDC), Cholesterol, NMD loaded-biolosomes, NMD-loaded biolosomes gels

X-ray diffraction (XRD) studies

View Article Online
DOI: 10.1039/D4NA00510D

Figure 10: XRD images of optimized bilosomes, NDP-loaded gel, cholesterol, Span® 60, and SDC. The crystalline NDP molecule exhibits peaks at 2, 6.2, 11.7, 14, 17.7, 19.4, 20.3, 21.4, and 22.2. SDC, unlike Span 60, displays crystalline peaks at various intensities (2, 3.2, 3.5, 3.7, 4, 4.5, 4.8, 5.3, 5.7, 6.5, 7, 7.6, 8.6, 9.8, 11.4, 17.4). Peaks in crystalline cholesterol occur at 6, 9, 11, 14, 16, and 21 2. Bilosome X-ray diffractograms showed Span 60's strong peak at 24 °C displaced. NDP crystallinity decreased in the optimized bilosome gel's X-ray diffractogram, showing fewer drug peaks. This demonstrates nanovesicle NDP.

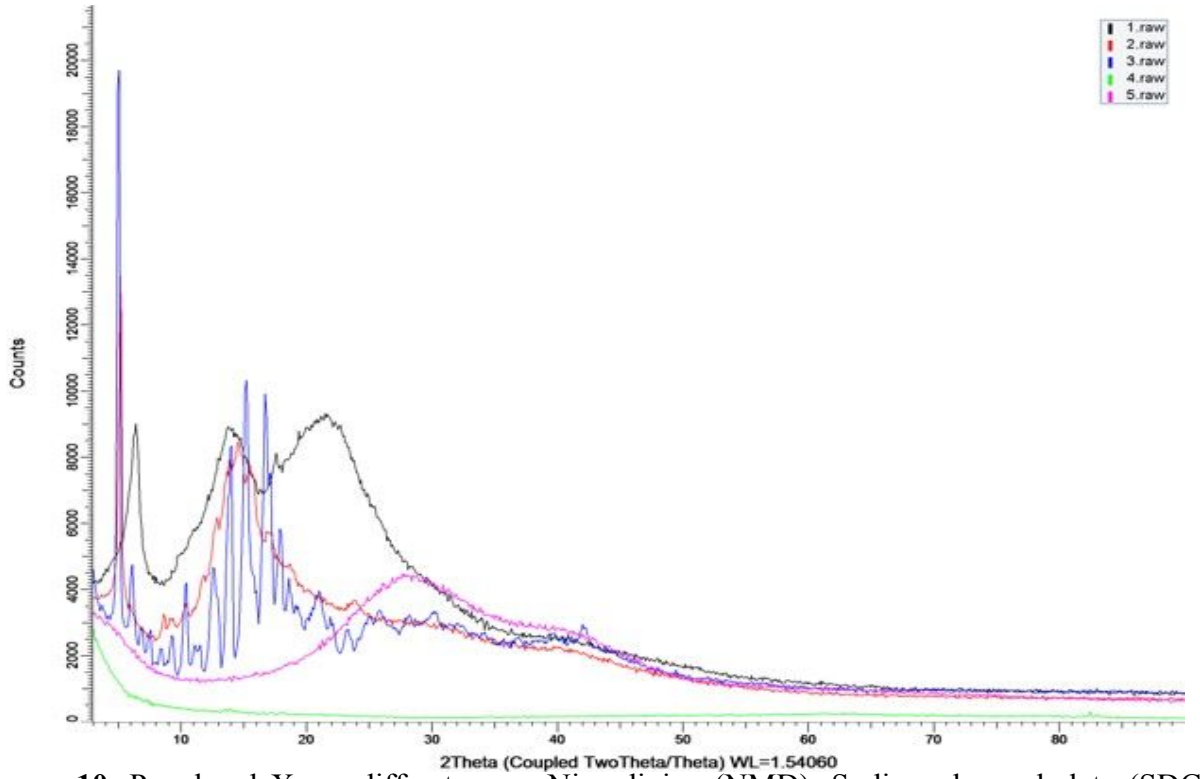

Figure 10. Powdered X-ray diffractogram Nimodipine (NMD), Sodium deoxycholate (SDC), NMD-loaded biolosomes, NMD-loaded biolosomes gels

Morphological Characterizations

After optimization, SEM revealed that NDP-bilosomes were smooth, spherical, and did not mix. Figure 11 shows SEM-imaged medicine and excipient surfaces. Peyer's patches are so small that they can move bilosomes to the intestinal lymphatic system. This way, the medicine can reach more cells without going through the liver. Malvern's particle size measurement differs from SEM's. SEM measures a nanoparticle's actual size, while DLS measures its hydrodynamic size. Smooth, spherical particles are best for lymphatic channels and cell transfer. Transmission electron microscopy corroborated photon correlation spectroscopy. Figure 12 demonstrates that Zetasizer

View Article Online
DOI: 10.1039/D4NA00510D

and TEM micrograph vesicle sizes were similar. Both NDP-loaded bilosomes and bilosomal gel formulations had smooth, spherical vesicles. AFM and TEM inspections indicated that the bilosome vesicles were consistently dispersed and spherical. Vesicle particle sizes were 150–170 nm, consistent with DLS (Dynamic light scattering) results. The lipidic vesicle's reaction with the mica substrate of the sample plate is shown in Figure 13. This probably led to larger, clustered vesicles in the (Atomic force microscopy) AFM spectrum.

Figure 11. Images of SEM (i) NMD-loaded biolosomes (ii) NMD-loaded biolosomes gels

.

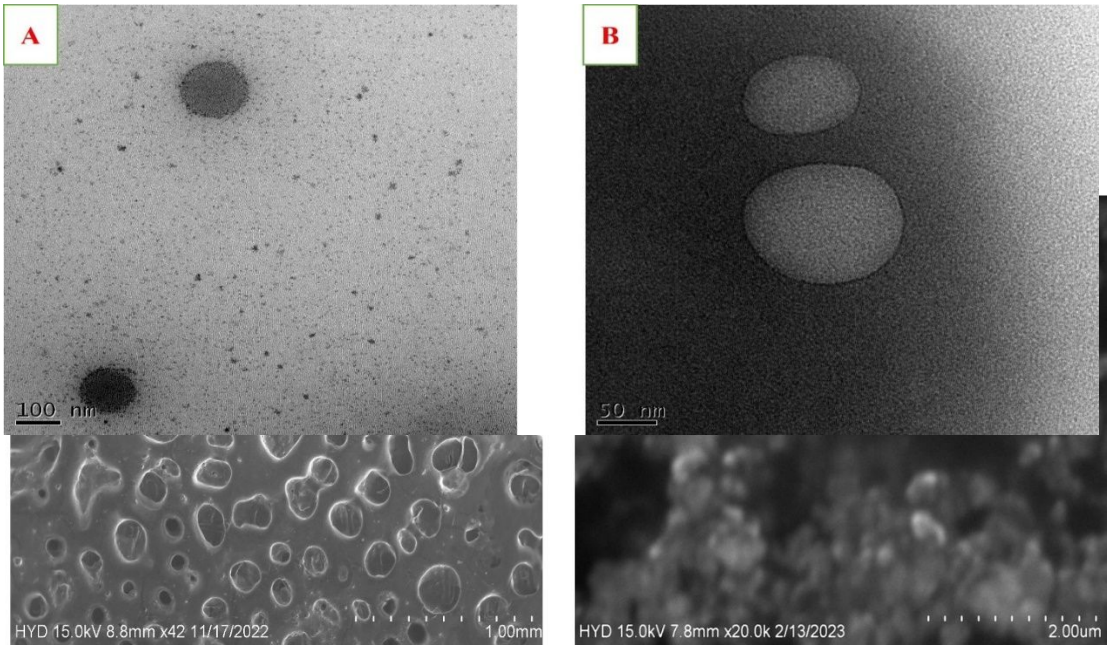

Figure 12. Transmission Electron Microscope images of (i) NMD-loaded biolosomes and (ii) NMD-loaded biolosomes gels.

View Article Online
DOI: 10.1039/D4NA00510D

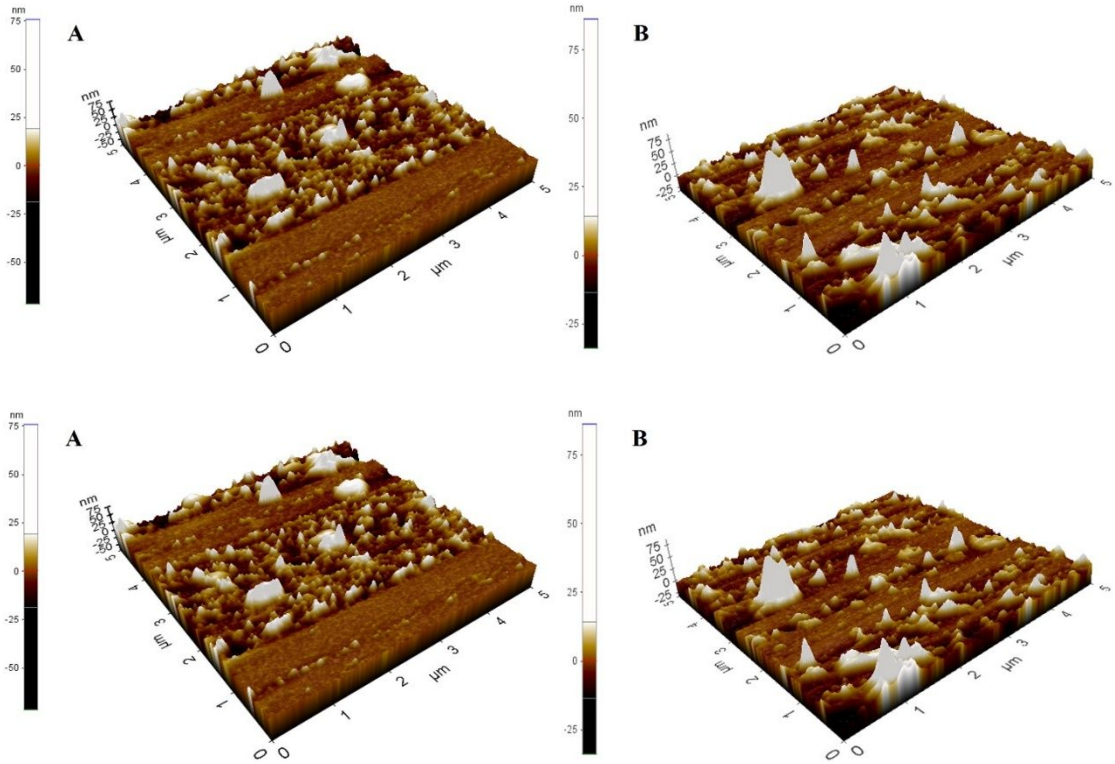

Figure 13. Atomic Force Microscopy images of (A& B) NMD-loaded biolosomes and (A&B) NMD-loaded biolosomes gels

In-vivo studies

Histopathology While alive, NDP bilosome suspension and NDP-loaded bilosomal gel did not alter the histology of skin layers in Groups II, III, and IV compared to the untreated skin slices in the control group (Figure 14). In the treated skin samples, all typical skin features were present. These findings demonstrated that NDP-loaded bilosomes were skin-safe.

View Article Online
DOI: 10.1039/D4NA00510D

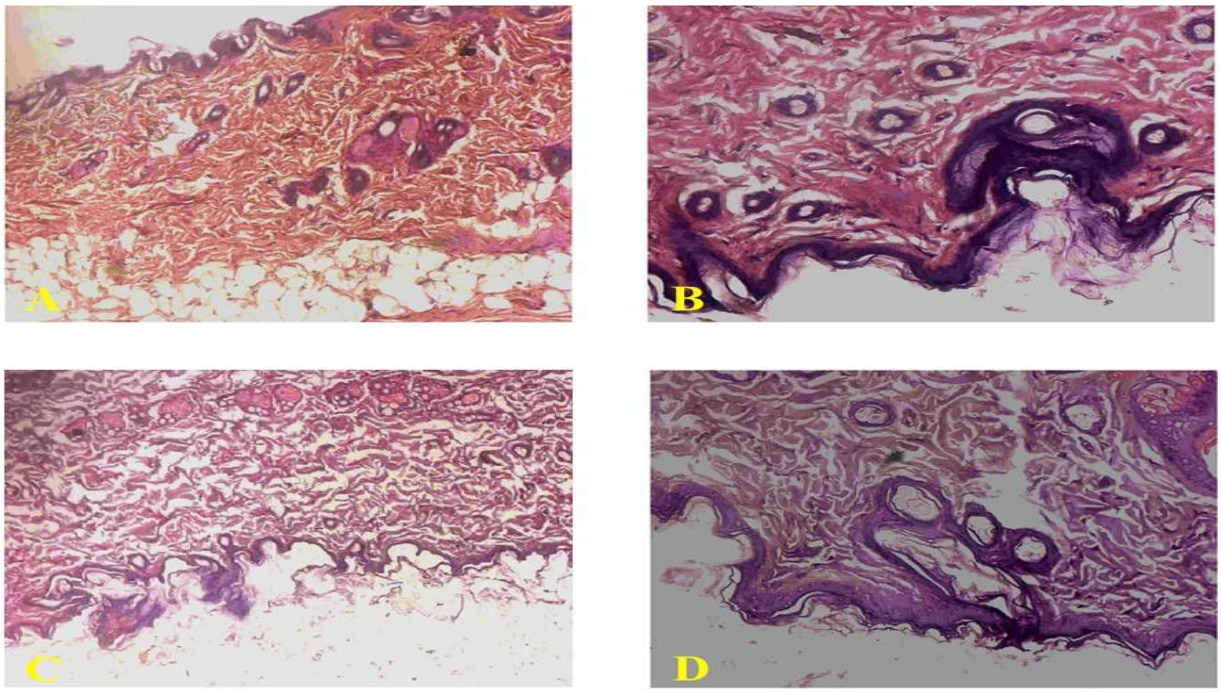

Figure 14. Shows photomicrographs of histopathological sections stained with hematoxylin and eosin. The sections depict the skin of rats in three different groups: group I-untreated, group II given with a suspension of NDP-bilosomes, and roup III and IV, which were treated with a marketed formulation of NDP-loaded bilosomal gel.

In-vivo skin deposition

In vivo, NDP from bilosomes and bilosomal gel deposited more into the skin than NDP solution (Figure 15). The topically applied NDP drug solution, NDP-bilosomes, and NDP-bilosomal gel groups had significantly different AUC0-10s ($p < 0.05$). AUC0-10 values for NDP-loaded bilosomal gel (654.32±69.85 μgh/cm^2) and 2.38 and 5.21 times more dispersion (298.67±15.23 μgh/cm^2) were compared. Compared to bilosomes and drug solution, NDP bilosomal gel was better. According to elasticity data, Bilosomes, which are particularly flexible, can self-divide dermal layers NDP and penetrate deeply due to bilosomal gel's improved skin deposition potential. Alternate skin features help transmit material across the skin, and intact and severely deformed vesicles must pass through the SC. SC contains lipids and proteins. Bilosomes may increase vesicle penetration by solubilizing membrane proteins and phospholipids. NDP accuracy also decreased over time. The skin's cellular absorption may have reached a saturation point, resulting in less drug deposition: more NDP in the circulation than in the dermis.

View Article Online
DOI: 10.1039/D4NA00510D

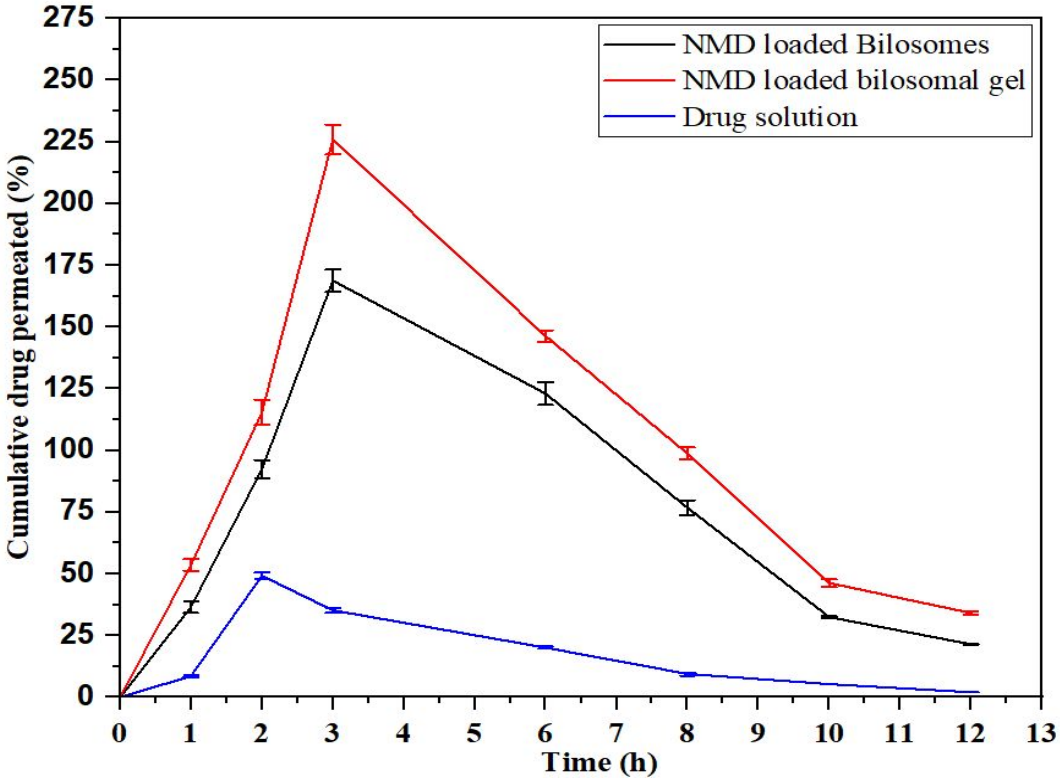

Figure 15. A time-dependent in-vivo skin deposition profile of NDP from bilosomes, bilosomal gel, and NDP solution following topical administration. The data is displayed as the mean ± standard deviation (n=3).

Pharmacokinetics Study of NDP Bilosomal Gel

Calculating the Pharmacokinetic Parameters

We compared oral NDP solution to NDP-bilosomal gel and NDP-bilosomes to assess bioavailability and pharmacokinetics experiments on rats. We administered gel, dispersion, and oral NDP to eight animals. Each animal's plasma NDP levels were tested. NDP bilosomal gel did not cause the group redness, pain, or swelling; their skin looked normal with distinct dermal and epidermal layers. The horny layer's thickness and appearance matched the control samples. These data confirm bilosomal system safety and tolerability. We evaluated the NDP bilosomal gel's plasma concentration-time curve against NDP oral solution. Averages and standard errors are included in pharmacokinetic and bioavailability data. Table 7 displays the average plasma NDP content in mg/mL, measured in hours following the administration of bilosomal gel in eight rats. Figure 16 shows the time-dependent mean plasma NDP concentration graph. We created it using the pharmacokinetic characteristics of an optimized transdermal NDP bilosomal gel and an oral

View Article Online
DOI: 10.1039/D4NA00510D

NDP suspension. The oral NDP suspension had a Cmax concentration of 52.37 µg/mL after 2 hours of administration, while the NDP bilosomal gel had 215.39 µg/mL after 16 hours. When the bilosomal gel was put on the skin, it released 67.21082238 (µg.h/mL) of NDP over time, while the oral therapy only released 0.439769476 (µg.h/mL). The SC barrier may explain why transdermal NDP has a higher tmax than oral NDP. The SC barrier hinders the penetration of NDP. Oral suspension seemed to release its contents faster. Bilosomal NDP gel outperformed oral NDP solution in mean $AUC_{0-\infty}$. When applied topically, NDP bilosomes could skip the first step of being processed by the liver, which may explain why they were more bioavailable. Because of its continuous release, the bilosomal gel's biological half-life increased from 2.84 to 3.01 hours compared to orally given medication. Half-life was longer after transdermal NDP administration due to prolonged absorption. Thus, the long-term drug-administration NDP bilosomal gel was established. Bilosomes serve as carriers and regulated release systems, which may explain the continuous release effect. NDP bilosomes improved gel bioavailability compared to oral solutions. Bilosomal formulations are lipophilic, which may increase absorption. We can use the mean pharmacokinetic characteristics to construct an NDP gel with high bioavailability and prolonged release activity using NDP bilosomes.

Table 3. Pharmacokinetic characteristics of NDP in rats following oral drug solution, bilosome, and bilosomal gel administration

Parameters	NDP-loaded Bilosomes	NDP-loaded Bilosomal gel	NDP solution
slope	-0.059517335	0.00581446	-0.098737239
intercept	0.205259211	0.00581446	-0.034141408
Ke	-0.137068422	0.013390701	-0.227391862
t1/2	-5.055869113	51.75233323	-3.047602472
C0	1.604202583	1.013478313	0.924397137
V_d	24934.50666	39468.03745	43271.44515
	24.93450666	39.46803745	43.27144515
clearance	-3417.733475	528.504673	-9839.574475
AUC o to t	1.302101292	1.006739156	0.962198568
AUC I to t	14.85	18.65	3.8
AUC t to infit	-0.729562643	67.21082238	-0.439769476

View Article Online
DOI: 10.1039/D4NA00510D

AUC total	15.42253865	86.86756154	4.322429092
Cmax	145.37	215.39	52.37
Tmax	3.02	3.64	2.38

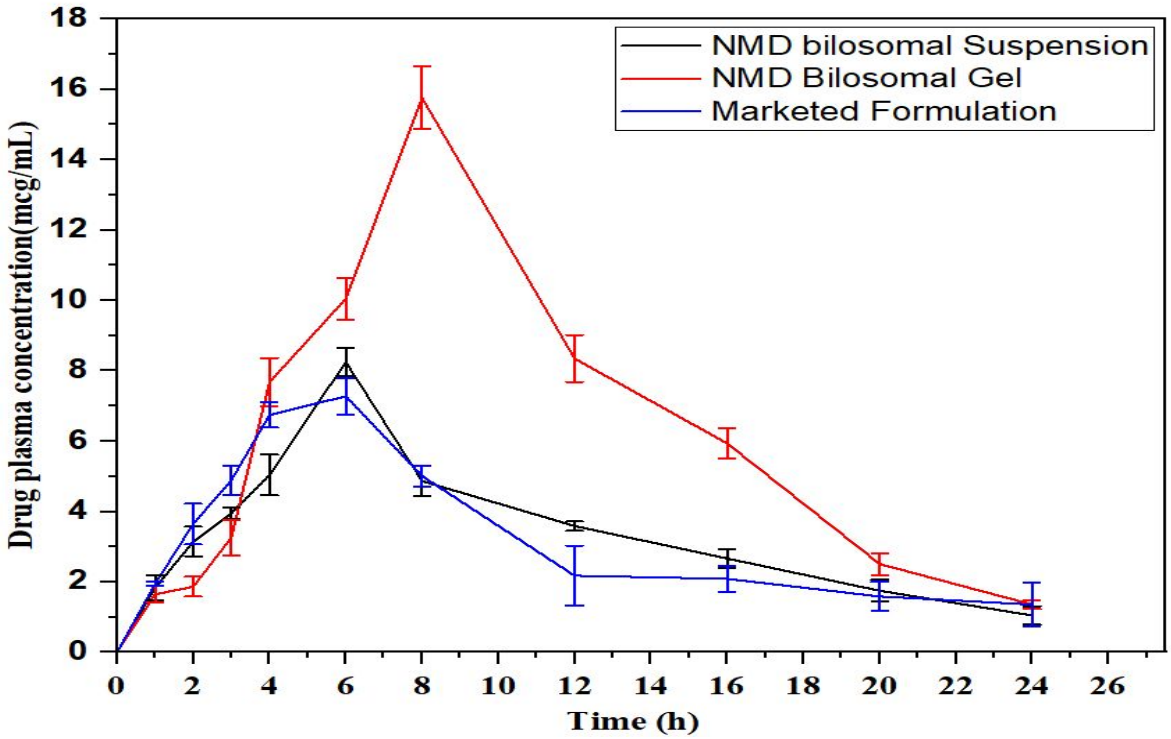

Figure 16. NDP-loaded bilosomes, oral drug solutions, and bilosomal gels: *in vivo* skin deposition profiles

In-vivo pharmacodynamic study

Transdermal application of an optimized bilosomal gel into hypertensive animals' dermis reduced blood pressure (BP). At 1, 2, 4, and 6 hours post-treatment, the normal control group, oral tablet, bilosomal solution, and NDP bilosomal gel groups had similar antihypertensive effects. Oral pills did not normalise blood pressure at 6, 8, and 12 hours post-treatment (Table 5). Transdermal bilosomal gel normalized blood pressure (BP) for 12 hours, with a maximum percentage reduction of 32.46 at 24 hours. Both oral tablet and bilosomal gel groups showed elevated blood pressure at 8 and 12 hours, but the difference was significant ($p<0.05$). After 8 and 12 hours, oral pills reduced BP by 0.86 and 2.67 per cent, whereas bilosomal gel reduced it by 18.94 and 10.52 per cent. Post-hoc analysis showed no significant change in the normal control or bilosomal gel groups ($p > 0.05$). Oral tablet groups showed significant differences ($p<0.05$) from the control group at 6, 8, and 12

View Article Online
DOI: 10.1039/D4NA00510D

hours post-treatment. NDP-bilosome surfactant moieties may limit mononuclear phagocyte NDP clearance *in vivo*, explaining the results. PBs maintained rat blood pressure for a longer time than pills.

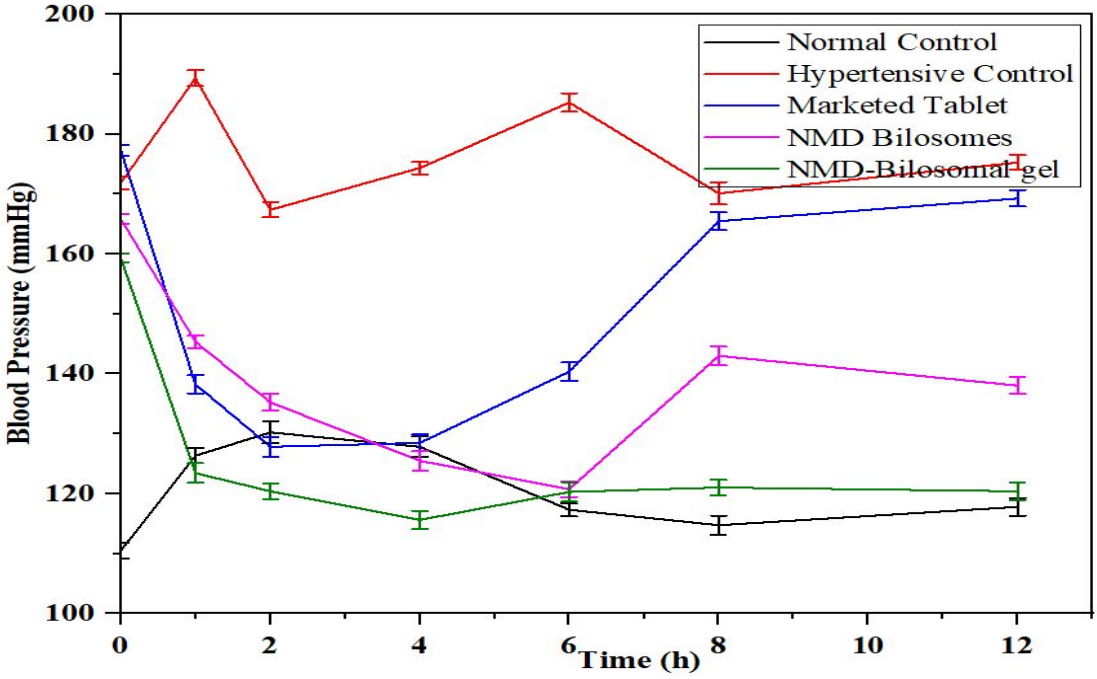

Figure 17. Oral medication solution, NDP-loaded Bilosomes, and Bilosomal gel anti-hypertensive potential

Conclusion

This study created bilosomes for transdermal NDP delivery. Ultrasonication following the "thin film hydration method" improved NDP-bilosomal formulations. The preliminary screening study was successful. Our research and development results and an evaluation of all factors led us to choose SDC as the surfactant and bile acid, with cholesterol added for penetration. Bile acid improves ZP and PS. A 3^3-factorial experiment yielded F4, the best formula. It had a small PS, a spherical form, and a high drug EE%. F4 penetrated better than NDP suspension in ex vivo studies. Histological analysis confirmed F4's tolerability. NDP was retained more in F4 rats' skin than drug suspension and bilosome dispersion in *in-vivo* skin deposition studies. F4 had a controlled and long-lasting effect on hypertensive rats. A pharmacokinetic study found that F4 increased NDP bioavailability compared to oral tablets. Because it addresses NDP's oral problems and has a high first-pass metabolism, F4 was considered a viable TDDS for NDP.

View Article Online
DOI: 10.1039/D4NA00510D

List of Abbreviations

NDP: nimodipine, SC: stratum corneum, TDDS: transdermal drug delivery system, HMC: hydroxymethylcellulose, SDC: sodium deoxycholate, TFH: Thin-film hydration, SAA: surfactant, CH: cholesterol, ANOVA: analysis of variance, PS: Particle size, ZP: Zeta potential, FTIR: Fourier Transform Infrared Spectroscopy, DSC: Differential scanning calorimetry, SEM: Scanning electron microscopy, TEM: Transmission Electron Microscopy, XRD: X-ray diffraction, DLS: Dynamic light scattering, AFM: Atomic force microscopy, BP: blood pressure.

Declarations

Acknowledgment

The authors thank to Kampala International University and Galgotias University for supporting this research work.

Ethics approval

Under the Society of Toxicology USP 1989 criteria, no animals were harmed during this study. The method was accepted by Jeeva life sciences' Institutional Animal Ethics Committee (IAEC) before the study began. Uppal, Hyderabad, India (Approval No.: CPCSEA/IAEC/JLS/011/11/23/16).

Funding

The author(s) received no specific funding for this work.

Disclosure statement

All authors report that there was no conflict of interest in this work.

Availability of data and materials

The datasets/information used for this study is available on reasonable request.

Author contributions

Conceptualisation: Sarad Pawar Naik Bukke and Ananda Kumar Chettupalli, Methodology and investigation: Sarad Pawar Naik Bukke, Ananda Kumar Chettupalli, Marati Kavitha, Tenpattinam Shanmugam Saraswathi and Shaik Abdul Rahaman; Analysis, interpreted the data and writing—original draft preparation: Sarad Pawar Naik Bukke, Ananda Kumar Chettupalli, Godswill James Udom, Marati Kavitha, Tenpattinam Shanmugam Saraswathi, Shaik Abdul Rahaman, Sachchida Nand Rai, Marati Kavitha, Narender Boggula, Narayana Goruntla, Tadele Mekuriya Yadesa,

View Article Online
DOI: 10.1039/D4NA00510D

Hope Onohuean.Writing—review and editing: Sarad Pawar Naik Bukke, Ananda Kumar Chettupalli, Godswill James Udom, Sachchida Nand Rai, Tadele Mekuriya Yadesa and Hope Onohuean. The authors read and approved the final manuscript.

Conflicting interest

All authors report that there was no conflict of interest in this work.

References

1 Panchagnula R., *Indian journal of pharmacology*, 1997, **29**, 140–156.
2 Y. Chen, M. Wang and L. Fang, *Drug Deliv*, 2013, **20**, 199–209.
3 W. Fong Yen, M. Basri, M. Ahmad and M. Ismail, *ScientificWorldJournal*, 2015, **2015**, 495271.
4 D. I. J. Morrow, P. A. McCarron, A. D. Woolfson and R. F. Donnelly, *TODDJ*, 2007, **1**, 36–59.
5 R. Muzzalupo, L. Tavano, R. Cassano, S. Trombino, T. Ferrarelli and N. Picci, *Eur J Pharm Biopharm*, 2011, **79**, 28–35.
6 E. Zarenezhad, M. Marzi, H. T. Abdulabbas, S. A. Jasim, S. A. Kouhpayeh, S. Barbaresi, S. Ahmadi and A. Ghasemian, *J Funct Biomater*, 2023, **14**, 453.
7 I. T. Mendes, A. L. M. Ruela, F. C. Carvalho, J. T. J. Freitas, R. Bonfilio and G. R. Pereira, *Colloids Surf B Biointerfaces*, 2019, **177**, 274–281.
8 A. M. Al-Mahallawi, A. A. Abdelbary and M. H. Aburahma, *Int J Pharm*, 2015, **485**, 329–340.
9 E. Zarenezhad, H. T. Abdulabbas, M. Marzi, E. Ghazy, M. Ekrahi, B. Pezeshki, A. Ghasemian and A. A. Moawad, *Antibiotics (Basel)*, 2022, **11**, 1208.
10 G. P. Kushla, J. L. Zatz, O. H. Mills and R. S. Berger, *J Pharm Sci*, 1993, **82**, 1118–1122.
11 H. Marwah, T. Garg, A. K. Goyal and G. Rath, *Drug Deliv*, 2016, **23**, 564–578.
12 A. M. Al-Mahallawi, O. M. Khowessah and R. A. Shoukri, *Int J Pharm*, 2014, **472**, 304–314.
13 Uchegbu, I.F and Vyas, S.P, *International Journal of Pharmaceutics*, 1998, **172**, 33–70.
14 R. Agarwal, O. P. Katare and S. P. Vyas, *Int J Pharm*, 2001, **228**, 43–52.
15 P. L. Honeywell-Nguyen and J. A. Bouwstra, *Drug Discov Today Technol*, 2005, **2**, 67–74.
16 A. Manosroi, L. Kongkaneramit and J. Manosroi, *Int J Pharm*, 2004, **270**, 279–286.
17 C. Sinico, M. Manconi, M. Peppi, F. Lai, D. Valenti and A. M. Fadda, *J Control Release*, 2005, **103**, 123–136.
18 A. Madni, M. A. Rahim, M. A. Mahmood, A. Jabar, M. Rehman, H. Shah, A. Khan, N. Tahir and A. Shah, *AAPS PharmSciTech*, 2018, **19**, 1544–1553.
19 A. Pardakhty, J. Varshosaz and A. Rouholamini, *Int J Pharm*, 2007, **328**, 130–141.
20 S. Ghanbarzadeh and S. Arami, *Biomed Res Int*, 2013, **2013**, 616810.
21 H. M. Aboud, A. A. Ali, S. F. El-Menshawe and A. A. Elbary, *Drug Deliv*, 2016, **23**, 2471–2481.
22 M. L. González-Rodríguez, C. M. Arroyo, M. J. Cózar-Bernal, P. L. González-R, J. M. León, M. Calle, D. Canca and A. M. Rabasco, *Drug Dev Ind Pharm*, 2016, **42**, 1683–1694.
23 D. Singh, M. Pradhan, M. Nag and M. R. Singh, *Artif Cells Nanomed Biotechnol*, 2015, **43**, 282–290.
24 S. Ahmed, M. A. Kassem and S. Sayed, *Int J Nanomedicine*, 2020, **15**, 9783–9798.

View Article Online
DOI: 10.1039/D4NA00510D

25 X.-Q. Niu, D.-P. Zhang, Q. Bian, X.-F. Feng, H. Li, Y.-F. Rao, Y.-M. Shen, F.-N. Geng, A.-R. Yuan, X.-Y. Ying and J.-Q. Gao, *Int J Pharm X*, 2019, **1**, 100027.
26 Y. Zhang, Q. Jing, H. Hu, Z. He, T. Wu, T. Guo and N. Feng, *Int J Pharm*, 2020, **580**, 119183.
27 A. P. Pandit, S. B. Omase and V. M. Mute, *Drug Deliv Transl Res*, 2020, **10**, 1495–1506.
28 L. Maione-Silva, E. G. de Castro, T. L. Nascimento, E. R. Cintra, L. C. Moreira, B. A. S. Cintra, M. C. Valadares and E. M. Lima, *Sci Rep*, 2019, **9**, 522.
29 A. Zafar, N. K. Alruwaili, S. S. Imam, N. Hadal Alotaibi, K. S. Alharbi, M. Afzal, R. Ali, S. Alshehri, S. I. Alzarea, M. Elmowafy, N. A. Alhakamy and M. F. Ibrahim, *Saudi Pharm J*, 2021, **29**, 269–279.
30 S. F. El Menshawe, H. M. Aboud, M. H. Elkomy, R. M. Kharshoum and A. M. Abdeltwab, *Drug Deliv Transl Res*, 2020, **10**, 471–485.
31 R. M. Khalil, A. Abdelbary, S. Kocova El-Arini, M. Basha and H. A. El-Hashemy, *J Liposome Res*, 2019, **29**, 171–182.
32 R. Albash, M. A. El-Nabarawi, H. Refai and A. A. Abdelbary, *Int J Nanomedicine*, 2019, **14**, 6555–6574.
33 N. A. Peppas, P. Bures, W. Leobandung and H. Ichikawa, *Eur J Pharm Biopharm*, 2000, **50**, 27–46.
34 I. M. Abdulbaqi, Y. Darwis, N. A. K. Khan, R. A. Assi and A. A. Khan, *Int J Nanomedicine*, 2016, **11**, 2279–2304.
35 E. Zarenezhad, R. O. Saleh, M. Osanloo, A. Iraji, A. Dehghan, M. Marzi and A. Ghasemian, *Russ J Bioorg Chem*, 2024, **50**, 855–869.
36 Mehtap Saydam and Sevgi Takka, *Fabad Journal of Pharmaceutical Sciences*, 2007, **32**, 185–196.
37 N. Nishida, K. Taniyama, T. Sawabe and Y. Manome, *Int J Pharm*, 2010, **402**, 103–109.
38 A. Zafar, S. S. Imam, N. K. Alruwaili, M. Yasir, O. A. Alsaidan, S. Alshehri, M. M. Ghoneim, M. Khalid, A. Alquraini and S. S. Alharthi, *Gels*, 2022, **8**, 133.
39 Y. Dai, R. Zhou, L. Liu, Y. Lu, J. Qi and W. Wu, *Int J Nanomedicine*, 2013, **8**, 1921–1933.
40 Dimitrov DS, Li J, Angelova M, and Jain RK, *FEBS Letters*, 1984, **176:**, 398–400.
41 A. Ismail, M. Teiama, B. Magdy and W. Sakran, *AAPS PharmSciTech*, 2022, **23**, 188.
42 null Ameeduzzafar, J. Ali, A. Bhatnagar, N. Kumar and A. Ali, *Int J Biol Macromol*, 2014, **65**, 479–491.
43 D. E. Aziz, A. A. Abdelbary and A. I. Elassasy, *J Liposome Res*, 2019, **29**, 73–85.
44 A. A. Abdelbary and M. H. H. AbouGhaly, *Int J Pharm*, 2015, **485**, 235–243.
45 I. Scognamiglio, D. De Stefano, V. Campani, L. Mayol, R. Carnuccio, G. Fabbrocini, F. Ayala, M. I. La Rotonda and G. De Rosa, *Int J Pharm*, 2013, **440**, 179–187.
46 W. Zhang, X. Zhao, G. Yu and M. Suo, *J Biomater Sci Polym Ed*, 2021, **32**, 858–873.
47 M. Ansari, M. Kazemipour and M. Aklamli, *Int J Pharm*, 2006, **327**, 6–11.
48 Haigh, J.M. and Smith, E.W., *European Journal of Pharmaceutical Sciences*, 1994, **2**, 311–330.
49 M. P. Vinardell and M. Mitjans, *J Pharm Sci*, 2008, **97**, 46–59.
50 A. Rudra, R. M. Deepa, M. K. Ghosh, S. Ghosh and B. Mukherjee, *Int J Nanomedicine*, 2010, **5**, 811–823.
51 A. Unnisa, A. K. Chettupalli, T. Al Hagbani, M. Khalid, S. B. Jandrajupalli, S. Chandolu and T. Hussain, *Pharmaceuticals (Basel)*, 2022, **15**, 568.

View Article Online
DOI: 10.1039/D4NA00510D

52 H. A. Hazzah, R. M. Farid, M. M. A. Nasra, M. A. El-Massik and O. Y. Abdallah, *Int J Pharm*, 2015, **492**, 248–257.
53 P. R. Amarachinta, G. Sharma, N. Samed, A. K. Chettupalli, M. Alle and J.-C. Kim, *J Nanobiotechnology*, 2021, **19**, 100.
54 E. S. El-Leithy and R. S. Abdel-Rashid, *Journal of Drug Delivery Science and Technology*, 2017, **41**, 239–250.
55 A. A. Boseila, A. Y. Abdel-Reheem and E. B. Basalious, *PLoS One*, 2019, **14**, e0219752.
56 Y. R. Neupane, M. Srivastava, N. Ahmad, N. Kumar, A. Bhatnagar and K. Kohli, *Int J Pharm*, 2014, **477**, 601–612.
57 M. T. Rao, Y. S. Rao, V. Ratna J and K. Kumari Pv, *ijps*, , DOI:10.36468/pharmaceutical-sciences.708.
58 R. Albash, A. A. Abdelbary, H. Refai and M. A. El-Nabarawi, *Int J Nanomedicine*, 2019, **14**, 1953–1968.
59 A. Ahad, M. Aqil, K. Kohli, Y. Sultana and M. Mujeeb, *Artif Cells Nanomed Biotechnol*, 2016, **44**, 1002–1007.
60 L. Bajerski, R. C. Rossi, C. L. Dias, A. M. Bergold and P. E. Fröehlich, *AAPS PharmSciTech*, 2010, **11**, 637–644.
61 D. L. J. Alexander, A. Tropsha and D. A. Winkler, *J Chem Inf Model*, 2015, **55**, 1316–1322.
62 H. Abdelkader, S. Ismail, A. Kamal and R. G. Alany, *Pharmazie*, 2010, **65**, 811–817.
63 M. A. El-Nabarawi, R. N. Shamma, F. Farouk and S. M. Nasralla, *J Liposome Res*, 2020, **30**, 1–11.
64 L. S. De Lima, M. D. M. Araujo, S. P. Quináia, D. W. Migliorine and J. R. Garcia, *Chemical Engineering Journal*, 2011, **166**, 881–889.
65 R. DeLoach and N. Ulbrich, in *45th AIAA Aerospace Sciences Meeting and Exhibit*, American Institute of Aeronautics and Astronautics, Reno, Nevada, 2007.
66 A. Salama, H. A. El-Hashemy and A. B. Darwish, *Journal of Drug Delivery Science and Technology*, 2022, **69**, 103175.
67 A. Sankhyan and P. K. Pawar, *Daru*, 2013, **21**, 7.
68 R. M. Khalil, G. A. Abdelbary, M. Basha, G. E. A. Awad and H. A. El-Hashemy, *J Liposome Res*, 2017, **27**, 312–323.
69 A. Abd-Elbary, H. M. El-laithy and M. I. Tadros, *Int J Pharm*, 2008, **357**, 189–198.
70 D. Kumbhar, P. Wavikar and P. Vavia, *AAPS PharmSciTech*, 2013, **14**, 1072–1082.
71 G. Abdelbary, *Pharm Dev Technol*, 2011, **16**, 44–56.
72 A. Zafar, O. A. Alsaidan, S. S. Imam, M. Yasir, K. S. Alharbi and M. Khalid, *Gels*, 2022, **8**, 418.
73 N. S. El-Salamouni, R. M. Farid, A. H. El-Kamel and S. S. El-Gamal, *Int J Pharm*, 2015, **496**, 976–983.
74 N. I. Elsherif, R. N. Shamma and G. Abdelbary, *AAPS PharmSciTech*, 2017, **18**, 551–562.
75 G. H. Naji and F. J. Al Gawhari, *PHAR*, 2024, **71**, 1–7.
76 H. Peddapalli, G. V. Radha and S. K. Chinnaiyan, *Journal of Drug Delivery Science and Technology*, 2024, **92**, 105400.
77 G. M. El Zaafarany, G. A. S. Awad, S. M. Holayel and N. D. Mortada, *Int J Pharm*, 2010, **397**, 164–172.
78 R. C. Nagarwal, S. Kant, P. N. Singh, P. Maiti and J. K. Pandit, *J Control Release*, 2009, **136**, 2–13.
79 M. Yusuf, V. Sharma and K. Pathak, *Int J Pharm Investig*, 2014, **4**, 119–130.

View Article Online
DOI: 10.1039/D4NA00510D

80 G. A. Abdelbary and M. H. Aburahma, *J Liposome Res*, 2015, **25**, 107–121.
81 K. K. Patel, P. Kumar and H. P. Thakkar, *AAPS PharmSciTech*, 2012, **13**, 1502–1510.
82 F. A. Moawad, A. A. Ali and H. F. Salem, *Drug Deliv*, 2017, **24**, 252–260.
83 K. Ruckmani and V. Sankar, *AAPS PharmSciTech*, 2010, **11**, 1119–1127.
84 O. Bortolini, T. Bernardi, G. Fantin, V. Ferretti and M. Fogagnolo, *Steroids*, 2011, **76**, 596–602.
85 Y. Lang, B. Li, E. Gong, C. Shu, X. Si, N. Gao, W. Zhang, H. Cui and X. Meng, *Food Chemistry*, 2021, **334**, 127526.
86 M. K. Chourasia, L. Kang and S. Y. Chan, *Results Pharma Sci*, 2011, **1**, 60–67.

View Article Online
DOI: 10.1039/D4NA00510D

Availability of data and materials

The datasets/information used for this study is available on reasonable request.